8-13-1965

Isothermal and non-isothermal flow of air in a vertical tube.

John I. Vissers
University of Windsor

ISOTHERMAL AND NON-ISOTHERMAL FLOW

OF AIR IN A VERTICAL TUBE

BY

JOHN I. VISSERS

B. E., Nova Scotia Technical College, 1964

A Thesis
Submitted to the Faculty of Graduate Studies through the
Department of Mechanical Engineering in Partial
Fulfillment of the Requirements for the
Degree of Master of Applied Science
at the University of Windsor

Windsor, Ontario, Canada

1965

ABM 9826

APPROVED BY:

C. St Pierre

A. A. Nicol.

W. G. Colborne

127869

ABSTRACT

In this experimental investigation, the isothermal Langhaar entrance theory for air flow in pipes was confirmed. The effect of small temperature differences on the flow was studied and it was found that even a few degrees difference between inside and ambient temperature would result in a form of turbulent flow at Reynolds numbers as low as 500. The non-isothermal velocity ratio ($u_{max}/\bar{U}$) was studied for Reynolds numbers between 500 - 4000. The buoyancy effect tended to elongate the velocity profiles in all cases and in some cases the velocity ratio was found to exceed the isothermal ratio of 2.0 in the laminar region i.e. $N_{Re} < 2000$. The velocity profile development showed four distinct regions produced by the cooling effect, entrance region, cooling region, isothermal profile development and fully developed isothermal laminar flow. In the cooling region, the Nusselt number was observed to increase with Reynolds number, but varied only slightly with changing Grashof numbers.

ACKNOWLEDGEMENTS

The author would like to express his gratitude to the following: Professor W. G. Colborne for supervision and encouragement, Professor Griffiths for advice, Mr. R. Myers and Mr. O. Brudy for technical assistance and the National Research Council for financial assistance.

TABLE OF CONTENTS

LIST OF FIGURES

NOTATION

A = surface area of pipe, L^2

C = calibration constant for hot-wire

C_p = specific heat at constant pressure, $Q/M\theta$

d = sectional position measured from the wall of the pipe, L

$D=d_w$ = diameter of pipe, L

f = functional relation

g = acceleration due to gravity, L/t^2

h = film coefficient, $Q/L^2t\theta$

I_o = current in hot-wire, ma($V = 0$ fps)

I = current in hot-wire, ma($V = u$ fps)

k = thermal conductivity of air, $Q/Lt\theta$

L = length of pipe, L

L' = entrance length, L

P = pressure, F/L^2

q = rate of heat transfer through pipe wall, Q/t

r = coordinate in radial direction, measured from center of the pipe, L

R = radius of pipe, L

u = axial velocity component L/t

$\overline{U}$ = mean or average velocity L/t

t = temperature in degrees Fahrenhiet, θ

t_b = bulk temperature of the air, θ

t_i = entrance temperature, θ

t_m = mean temperature of the air, θ

t_o = ambient air temperature surrounding the pipe, θ

t_w = wall temperature of the pipe, θ

T = temperature in degrees absolute, θ

V = velocity of air, L/t

W = mass flow, M/t

x = axial distance from entrance of the pipe, L

N_{Gr} = Grashof number, $\frac{\rho^2 D^3 g \beta \Delta T}{\mu^2}$

N_{Gz} = Graetz number, $\frac{W C_p}{k L}$, $\frac{\pi}{4} N_{Re} N_{Pr} \frac{D}{L}$

N_{Nu} = Nusselt number, hD/k

N_{Pe} = Peclet number, $N_{Re} N_{Pr}$

N_{Pr} = Prandtl number, $C_p\mu/k$

N_{Re} = Reynolds number, $\rho\bar{U}D/\mu$

β = coefficient of thermal expansion, $1/T_o$, $1/\theta$

μ = absolute viscosity, M/Lt

Δ = difference of two values, or small increment

ρ = density of air, M/L^3

F = Force, pounds

L = Length, feet

M = Mass, pounds

Q = Heat, British Thermal Units

t = Time, seconds

θ = Temperature, Fahrenheit degrees

CHAPTER 1

INTRODUCTION

If experimentation is to be useful in the design of apparatus, the boundary conditions imposed on the experiment should approximate the boundary conditions of the actual apparatus. It is apparent, for instance, that in the design of certain heat exchangers and chimneys, the assumption of either constant wall temperature or constant heat flux does not approximate the actual conditions very closely. Some of this equipment would be more realistically designed on the basis of constant ambient temperature, and thus the following investigation was undertaken.

This investigation served to study both non-isothermal and isothermal flow of air in a vertical pipe. The air inside the pipe was cooled as it flowed upward, and the ambient air surrounding the pipe was assumed to be at constant temperature for any given test.

Since the Prandtl number change was found to be negligible, the constant value of 0.71 was used in this study.

Initially isothermal flow was studied to confirm Langhaar's entrance length relation. The velocity profile development was carefully studied for the non-isothermal case in order to determine the effect of heat transfer on this parameter.

CHAPTER 2

EXISTING THEORY AND EXPERIMENTAL RELATIONS

Isothermal

Two definite regions are present in fluid flow, laminar and turbulent. Although it is generally accepted theory that the critical Reynolds number, that is the transition between these two regions, is approximately 2100, much higher and lower values have been obtained experimentally. Also the transition is usually a fairly wide region in which the flow is intermittent. Experimental work by J. Rotta (15) showed the transition region to be between Reynolds numbers of 2300 - 2600, for his particular investigation, but it varies from one experiment to the next depending on conditions.

When a fluid such as air enters a pipe, a boundary layer builds up along the walls of the tube due to the viscosity of the fluid. At the entrance, the velocity profile will be flat, but further along the pipe the fluid near the wall will be slowed down due to the viscous forces. From the law of continuity this necessitates an increase in velocity at the center. The viscous or boundary layer will increase in thickness finally producing the parabolic profile in the case of laminar flow. At this point fully developed flow is obtained and assuming no disturbances, this condition will be maintain ed throughout the remainder of the pipe.

The length to produce this parabolic profile in laminar flow is called the settling or entrance length. For turbulent flow the settling length is shorter and the velocity profile flatter. Since this length is important in many engineering applications much analytical work has been done to predict it for pipes at any Reynolds number.

The equation for parabolic profiles is

$$\frac{v}{u_{max}} = 2\ [1 - (\frac{r}{R})^2\ ] \qquad (1)$$

Some investigators in this area have been Langhaar (10), Boussinesque (1) and Schiller (18), who obtained the following equations respectively:

$$\frac{L}{D} = 0.0575\ N_{Re} \qquad \text{where } N_{Re} = \frac{\rho DV}{\mu} \qquad (2)$$

$$\frac{x}{rN_{Re}} = 0.26 \qquad \text{where } N_{Re} = \frac{\bar{u}r}{\nu}$$

which is equivalent to

$$\frac{L}{D} = 0.065\ N_{Re} \qquad \text{where } N_{Re} = \frac{\rho DV}{\mu} \qquad (3)$$

and

$$\frac{x}{rN_{Re}} = 0.115 \qquad \text{where } N_{Re} = \frac{\bar{u}r}{\nu}$$

which is equivalent to

$$\frac{L}{D} = 0.028\ N_{Re} \qquad \text{where } N_{Re} = \frac{\rho DV}{\mu} \qquad (4)$$

The results of Langhaar and Boussinesque are in good agreement with the experimental data of Nikuradse, and as will be shown, with the present investigation, but Schiller's prediction was low.

The above expressions hold true only for laminar flow i.e. where the Reynolds number based on pipe diameter lies below 2000 - 3000.

According to McAdams (12), the ratio of maximum to average velocity, which is 2.0 for laminar flow, drops sharply to 1.38 between Reynolds numbers of 2100 - 3000 and from there on decreases more slowly with increasing Reynolds numbers. For turbulent flow, this ratio is approximately 1.2 and the Reynolds number at which this is obtained varies with different conditions.

Non-isothermal

Although much research has been done for non-isothermal flow of air in vertical pipes, the conditions varied considerably, and very little data is available for upflow with cooling. The common conditions of

1. Constant wall temperature
2. Constant heat flux
3. Uniform internal heat generation
4. Constant fluid properties

have been under consideration for many decades beginning with Graetz in 1885. Although many of the investigations were analytical, considerable experimental work has been done under these conditions. Due to the many variables to be considered, there does not seem to be one solution to cover this complex problem.

Yamagata (21), in 1940, was one of the first to consider variable properties when he published his analytical work including the effect of variable viscosity.

Deissler (3,4) derived equations to predict the radial velocity and temperature distributions including the effect of variable properties for turbulent flow. He concluded that this effect could be eliminated by evaluating the gas properties at a temperature close to the average of the wall and bulk temperature. To obtain the temperature at which to evaluate the properties he used $x(t_o - t_b) + t_b$, where x is an arbitrary number. Plotting N_{Nu} with t_o/t_b, he then selected that arbitrary number which made Nusselt number independent of t_o/t_b. For laminar flow the following temperature was thus selected:

$$t_{-0.27} = -0.27\,(t_o - t_b) + t_b$$

and the viscosity for the friction factor was evaluated at

$$t_{0.58} = 0.58\,(t_o - t_b) + t_b$$

where t_o is wall temperature, ^{o}R

t_b is the bulk temperature of the fluid at the cross section, ^{o}R.

Deissler also showed that the Nusselt numbers for laminar flow were independent of Reynolds and Prandtl numbers, but for turbulent flow it did depend on these two parameters. In another report, he predicted that the effect of variable properties for turbulent flow may be eliminated by evaluating the fluid properties at a temperature close to the average of the wall and bulk temperatures. He also noted that for laminar flow, heat addition elongated the velocity profile while for cooling it was flattened if natural convection effects were neglected. This was confirmed by Pigford (14) and McAdams (12).

R. L. Pigford (14) was the first to consider both variable viscosity and density in his analytical work. His results for constant wall temperature were confirmed by experimental data of Martinelli and Boelter (11) and Nikuradse. He calculated the effects of a distorted velocity profile on the heat transfer rate. He showed graphs of mean Nusselt number versus Graetz number and concluded that the Nusselt number was a function of Grashof modulus. Various ratios of wall to centerline viscosities were considered. He showed that the Nusselt number increased with Grashof modulus for any Graetz number. The Grashof modulus was defined as the product of Grashof number, Prandtl number and D/L ratio.

Nicoll and Kays (13) studied the effects of large temperature differences and found that the fluid properties varied enough to make the use of theoretical solutions based on constant properties invalid. This condition was studied for both laminar and turbulent flow in the fully developed region. The analytical solutions showed that the effect of large temperature differences was greatest for turbulent heating, while they were small for laminar heating and cooling and turbulent cooling. All the properties were evaluated at the mixed mean temperature for laminar heating, while for laminar cooling the logarithmic mean temperature with respect to end and wall temperature was used. For turbulent cooling the logarithmic mean temperature was also used. If the properties were evaluated at these temperatures, the effect of temperature on property variation was negligible, i.e. the Graetz solution seemed to predict the local Nusselt numbers correctly. For turbulent heating the theory did not hold but could be used if the Nusselt number was multiplied by $(T_w/T_m)^{0.5}$.

A. A. Szewczyk (20) investigated the effects of buoyancy forces on forced-convection laminar flow. Solutions were obtained by expanding the stream and temperature functions into series. This was done in terms of the parameter Gr_x/Re_x^2 when forced-convection was predominant, and in terms of the parameter $(Gr_x/Re_x^2)^{-1/2}$ when free-convection predominated. His work was done on a flat plate.

Hanratty et al (16,17) investigated the effect of heating and cooling of water at low Reynolds numbers. They noted that for heating with upflow the entering parabolic profile was distorted. The fluid at the center was decelerated while at the wall the velocity increased. The flow at the center was reversed and further downstream this region became unstable and initiated turbulence. For cooling the parabolic profile was elongated.

Gulati (6) studied the effects of variable fluid properties, and assuming a parabolic profile used a temperature profile which was determined experimentally, to calculate the velocity profile. He showed that buoyancy forces predominated, which elongated the velocity profile at the center.

Drobitch (5) investigated the non-isothermal flow of air in a vertical pipe. Using laminar flow and high entrance temperature, he concluded that

(1) A non-laminar motion existed for all non-isothermal runs, including those below a Reynolds number of 1000. This effect was noted even when the entrance temperature was but slightly higher than the ambient.

(2) For non-isothermal conditions the ratio $u_{max}/\bar{U}$ increased with increasing values of $\frac{T_m - T_o}{T_m}$ and decreasing Reynolds numbers. This ratio, however,

never reached 2.0 as expected for laminar flow.

(3) Above Reynolds numbers of 6000, the velocity profile was the same for isothermal as for non-isothermal flow.

The last two investigations are the only two available which apply to the present investigation.

From the literature it is evident that the temperature at which the properties of the air are evaluated is a major factor. So far many different temperatures have been used, three of the most popular are bulk mean temperature, log mean temperature and arithmetic mean temperature. They are expressed by the following equations respectively:

$$t_b = \frac{\int_0^{r_o} c_p \, t \, u \, r \, dr}{\int_0^{r_o} c_p \, u \, r \, dr}$$

$$t_{lm} = \frac{\Delta t_1 - \Delta t_2}{\ln \frac{\Delta t_1}{\Delta t_2}}, \quad \Delta t_1 = (t_w - t_m)_1$$

$$t_{am} = \frac{t_b + t_w}{2}$$

Since the calculation of Nusselt number, the most important parameter, includes these properties, (μ, k, ρ), its value will depend on which equation is chosen.

$$N_{Nu} = \frac{hD}{k}$$

where h, the film coefficient is

$$h = \frac{q}{A \, \Delta t}$$

where Δt is the difference between the bulk fluid temperature and wall temperature.

The coefficient of heat transfer h may be obtained by equating the following:

$$q = h A \Delta t$$

and

$$q = w \bar{C}_p \Delta t_b \qquad \bar{C}_p = \text{mean specific heat}$$

It may be shown that for forced convection

$$N_{Nu} = f(N_{Re}, N_{Pr})$$

while for free convection

$$N_{Nu} = f(N_{Gr}, N_{Pr})$$

If both free and forced convection are present then:

$$N_{Nu} = f(N_{Re}, N_{Gr}, N_{Pr})$$

Martinelli and Boelter (11) obtained the following expression:

$$N_{Nu} = 1.75\ F_1 \sqrt[3]{\frac{w\ C_{pb}}{k_b\ L} + .0722\ [\frac{D}{L},\ N_{Gr},\ N_{Pr}]_w^n\ F_2} \qquad (5)$$

where Grashof number was based on tube diameter and initial temperature difference which is always positive. The predicted exponent value (n) was 0.75.

The dimensionless factor F_1 was

$$F_1 = \frac{t_2 - t_1 / \Delta t_a}{\ln\left(2 + \frac{t_2 - t_1}{\Delta t_a} / 2 - \frac{t_2 - t_1}{\Delta t_a} \right)}$$

Values for F_2 were given in their results.

Knudsen and Katz (9) correlate the results of several investigators such as Hausen, Kraussold, Nusselt and Seider and Tate. Hausen deduced an equation by analytical means which states:

$$N_{Nu_m} = 3.66 + \frac{0.0668\ (x/d_w/Pe)^{-1}}{1 + 0.04\ (x/d_w/Pe)^{-2/3}} \qquad (6)$$

He considered constant wall temperature and a parabolic velocity distribution. Seider and Tate proposed the following equation:

$$N_{Nu_m} = 1.86 \left(\frac{x/d_w}{Pe}\right)^{-1/3} \left(\frac{\mu_b}{\mu_w}\right)^{0.14} \qquad (7)$$

where μ_b is the viscosity of the fluid at its arithmetic mean bulk temperature.

They also used constant wall temperature and considered the effects of variable viscosity, but natural convection was not taken into account. Oil was used instead of air.

CHAPTER 3

APPARATUS AND INSTRUMENTATION

This chapter will deal with the apparatus and instrumentation required to do this investigation. The necessary calibrations will be discussed here and presented in more detail in the appendix.

Basic Description

The furnace used was built for previous investigations (5,6). The required air was taken from the low pressure line available in the building. It was piped through a filter and pressure reducing valve combination from which it entered a high-accuracy flow meter. It then passed through a diverging section into the furnace where it could be heated to any desired temperature, by heating elements controlled by a variac. From here it entered the aluminum test pipe. The schematic layout is shown in Figure 1.

Flow Meters

The volume of air was controlled by valves and measured by means of two Brooks high accuracy flowmeters, whose accuracy was within one per cent. The range available was from zero to 10.5 standard cubic feet per minute at a pressure of 14.7 psia and 70° F. The low range flowmeter was capable of supplying 0 - 3.18 scfm and the high range from 1.0 to 10.50 scfm.

Furnace

The air entered the furnace through a sheet metal transition. To ensure uniform distribution of the air across the heating elements, a wire mesh screen was installed below them. The elements consisted of five Nichrome wire electric heaters, four of which were 3000 watts each, while the fifth, rating 2000 watts, was connected to a variac to provide control of the air temperature leaving the furnace. To reduce heat transfer to the surroundings, the furnace was covered with two inch thick magnesia blocks. Temperature and velocity profiles at the exit of the furnace were found to be flat.

Leakage

To determine leakage, the exit of the furnace was blocked. Then the maximum flow of air was forced into the furnace. A pressure reading in the pipe leading to the furnace would thus indicate the extent of air leaking out of the system. The furnace was sealed until the maximum leakage was below one per cent. Since the pressure within the furnace was many times higher under these conditions than under normal flow (unblocked exit) the leakage was assumed to be negligible.

Test Section

The test section consisted of a thirty-six foot aluminum pipe of two inch outside and 1.87 inches inside diameter. Twelve stations were located along its length to allow for the measurement of temperature and velocity profiles. These stations were located at: 0.25, 1.25, 4.5, 8.0, 11.0, 14.0, 17.5, 21.0, 25.0, 28.0, 31.0 and 34!0 feet from the entrance. The entrance to the test pipe was made up by a bell-mouth shaped aluminum section.

Temperature Measurement

The ambient air temperature was measured with an accurate thermometer, which was also used to measure the reference junction temperature of the potentiometer. The test pipe wall temperature and the temperature of the air at the station inside the pipe were measured by chromel constantan thermocouples. The thermocouple probe, to measure inside the pipe, was calibrated against an accurate thermometer (within 0.1%). All wall thermocouples were connected to a Thermovolt Instrument's 24 point rotary switch, which in turn was connected to a model 2745 Honeywell Potentiometer.

Pressure Measurement

The barometric pressure was read on a laboratory barometer, accurate to $\pm$ 0.01"Hg. For purpose of hot-wire calibration a Model MM3 Flow Corp. Micromanometer was used. It could be read to $\pm$ 0.0002" of the liquid (Butyl Alcohol) over a two inch range.

Hot-wire Anemometer

The hot-wire anemometer was used for all velocity readings. The Flow Corporation Model HWB3 was used. Each hot-wire used was calibrated in a specially designed calibrating unit. The method is well described in reference (5) and a brief explanation and typical curve is presented in Appendix A.

CHAPTER 4

EXPERIMENTAL RESULTS

The purpose of this investigation was to study the isothermal settling length and the non-isothermal heat transfer characteristics for air flow in a vertical pipe. Both laminar and turbulent runs were included to determine whether both were affected in the same manner. The temperature of the entering air was kept low to determine whether a small Δt would produce turbulence at low Reynolds numbers. Also the minimum temperature difference $(t_i - t_o)$ necessary to create this effect was investigated. A run at a high temperature difference was taken to compare with readings taken by A. J. Drobitch (5) and to see whether diameter affected the various heat transfer parameters. The weight flows were selected to cover a range of entrance Reynolds numbers from 500-4000. For isothermal runs, one hour was allowed for the system to reach steady state, while for non-isothermal conditions this period was extended to eight hours. The weight flow was readily set on the Brook's Instruments Hi-Accuracy flowmeters. Readings were taken only when the ambient air temperature difference along the pipe was within two degrees.

For each run the following readings were recorded:

(1) Barometric Pressure

(2) Ambient air temperature at every station along the axis of the pipe

(3) For non-isothermal runs the temperature profile at

each station

(4) Wall temperature at every station

(5) Velocity distribution at a minimum of three L/D ratios

(6) Inlet temperature

(7) Volume flow of air in the pipe.

Velocity Profiles

The variation of velocity ratios ($u_{max}/\bar{U}$) with L/D ratio for both isothermal and non-isothermal flow at Reynolds numbers from 500-4000 was measured. This is shown graphically in Figures 2, 6, 7, 8, 9 and 10, and is discussed in the next chapter.

Heat Transfer Results

The variation of mean temperature (t_m), wall temperature (t_w) and local Nusselt numbers with L/D ratios is shown in Figures 4 and 5 for Reynolds numbers of 500 and 3000. Values for these and all other Reynolds numbers are tabulated in Appendix C. The results are discussed in the next chapter.

Accuracy of Velocity Measurement

The accuracy of the velocity measurements was obtained by comparing the experimental mass flow obtained from the velocity readings with the mass flow obtained from the flowmeters. The accuracy was within 3.5%.

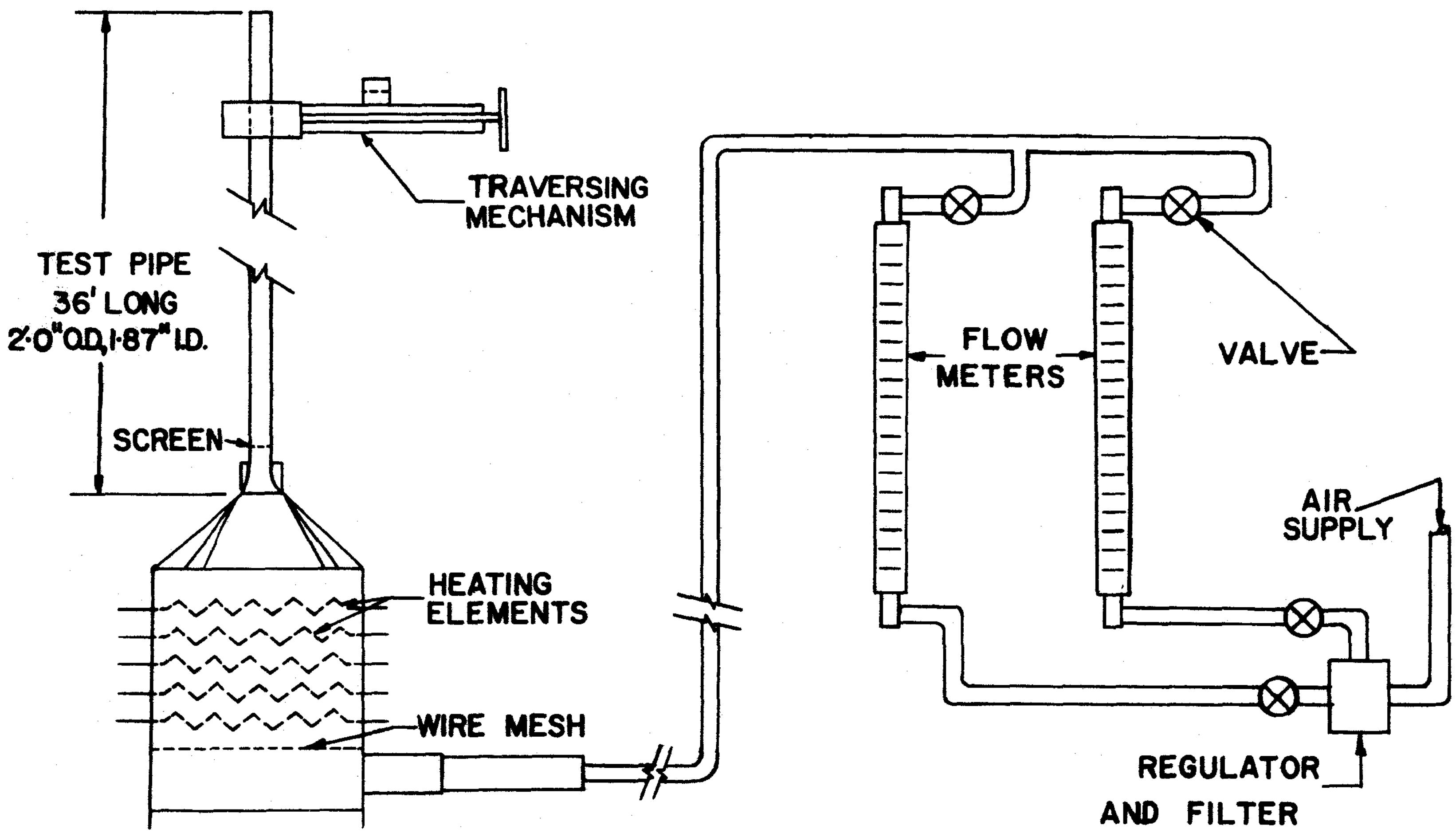

Fig. 1. Schematic layout of equipment (not to scale)

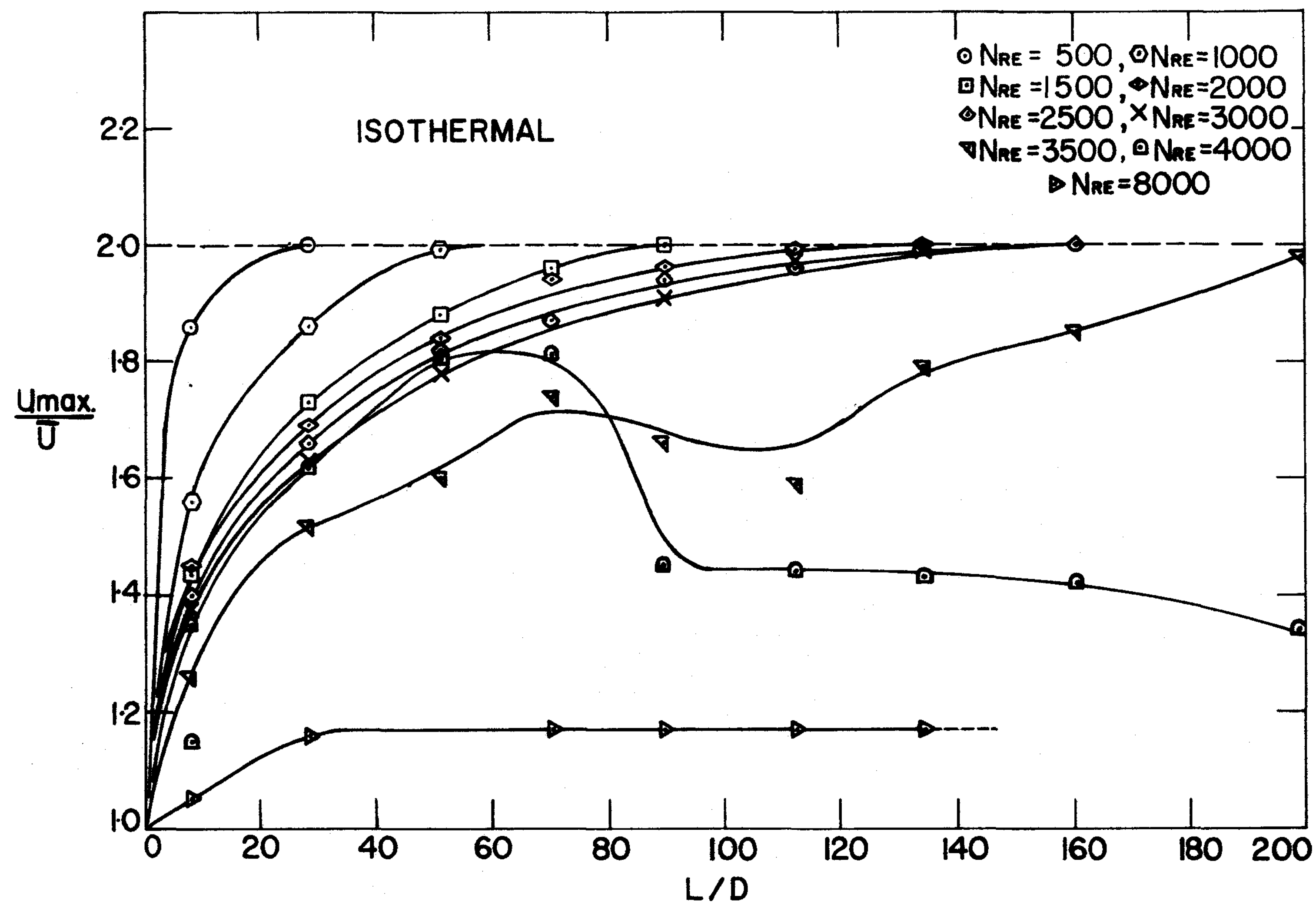

Fig. 2. Variation of $\frac{U_{max.}}{\bar{U}}$ with $\frac{L}{D}$ for isothermal flow

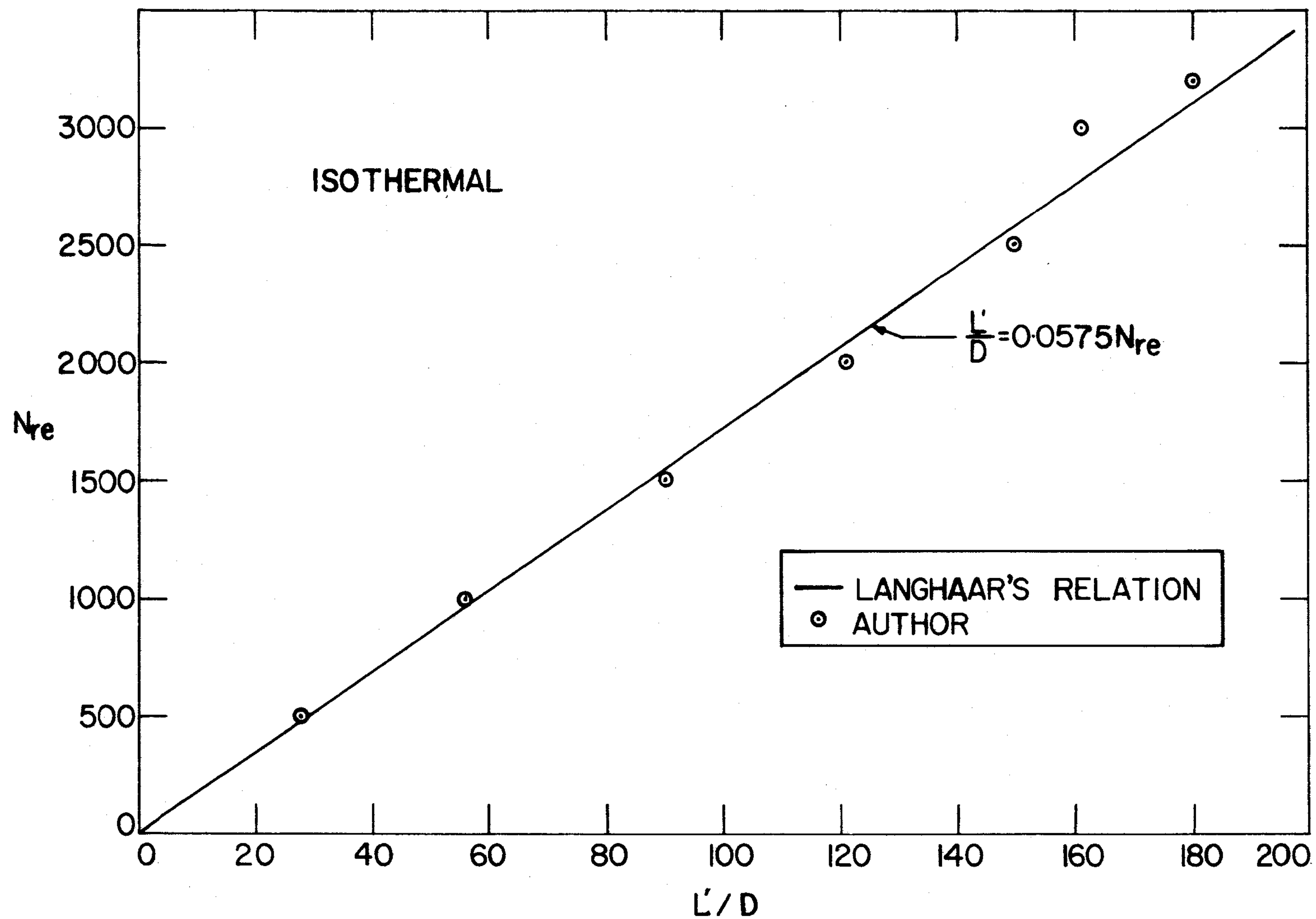

Fig. 3. Variation of entrance length with N_{re}

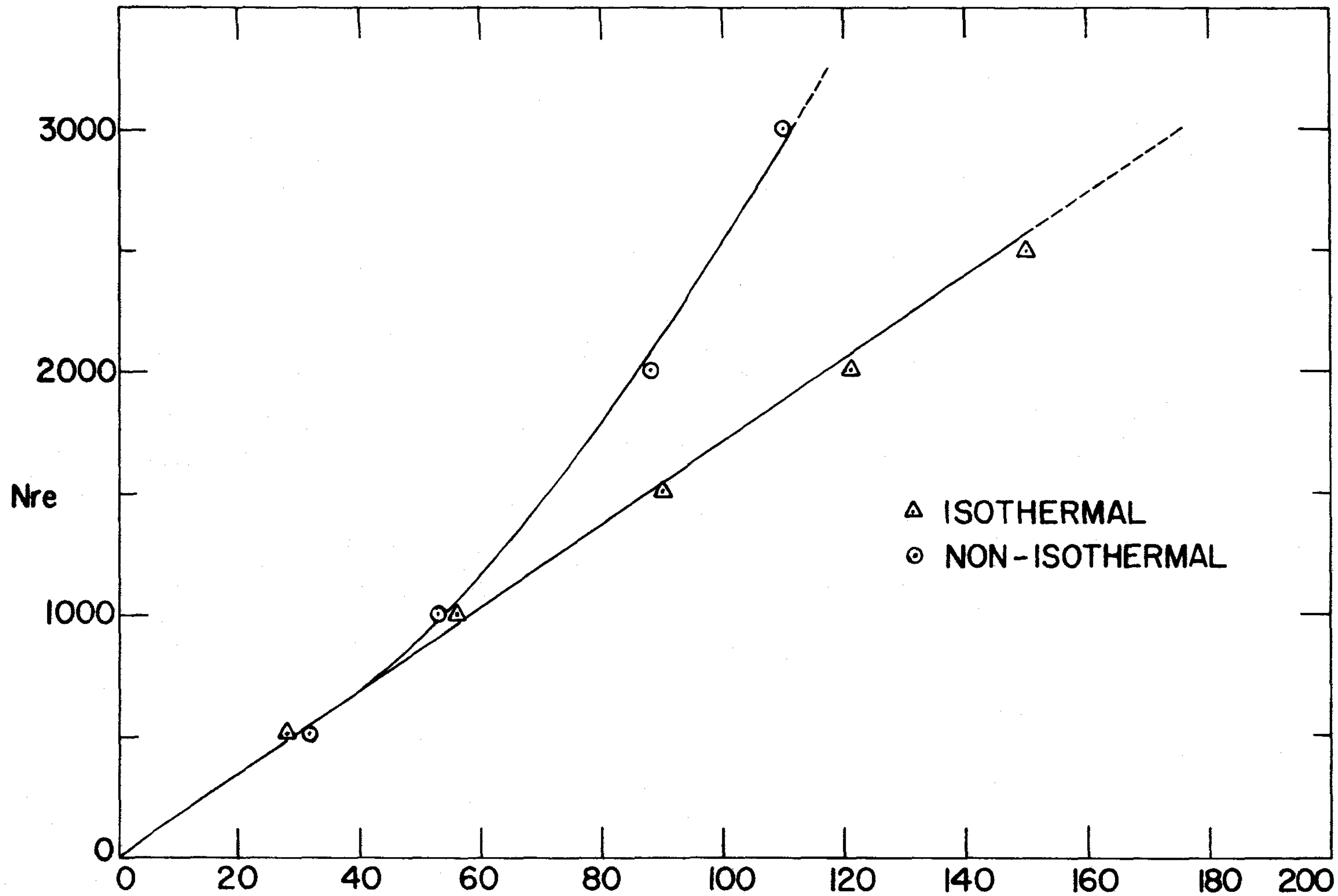

Fig. 3(a) Variation of entrance length with Nre for isothermal and non-isothermal flow

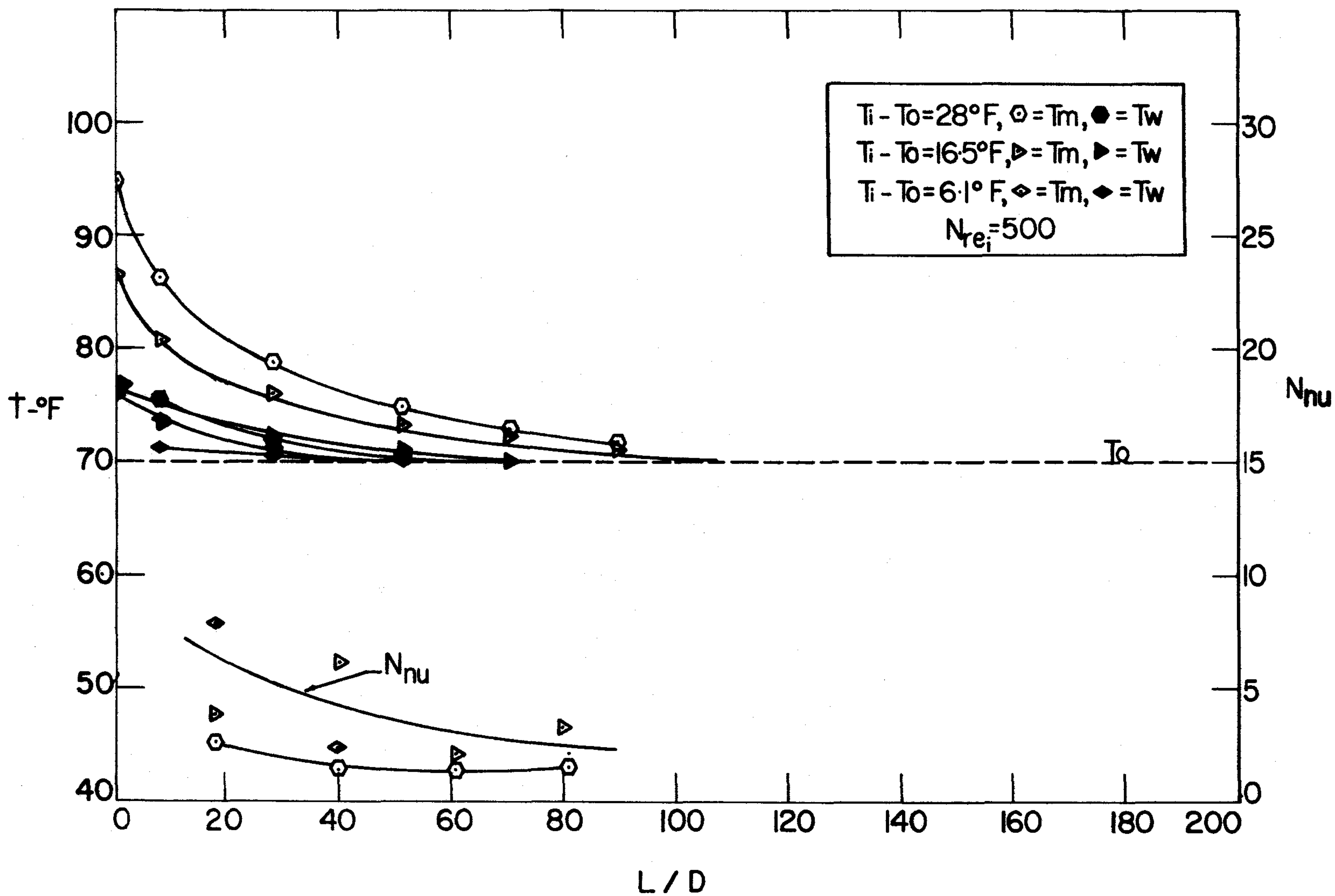

Fig. 4. Axial variation of temperatures and Nusselt numbers for $N_{re_i}=500$

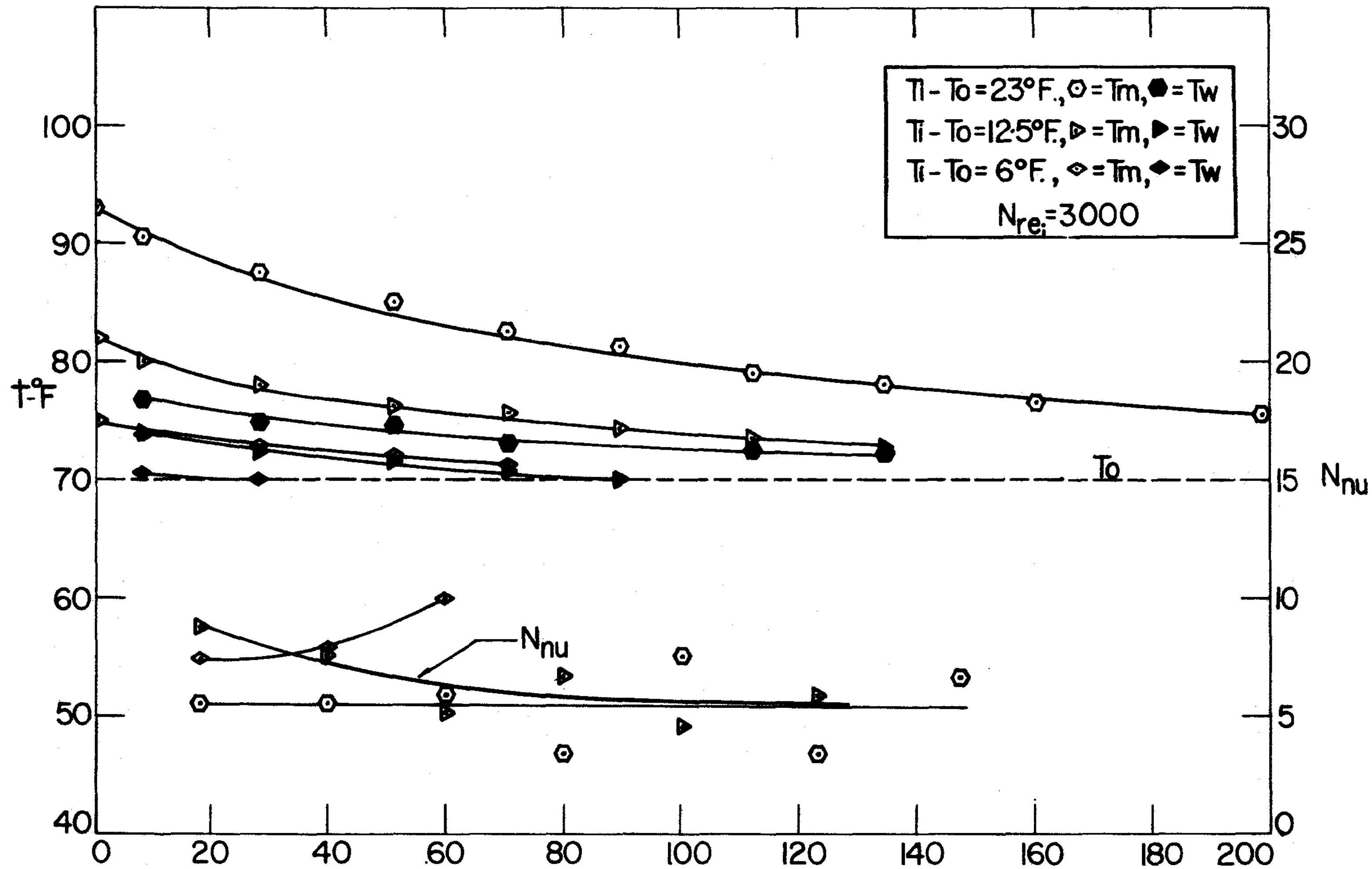

Fig. 5. Axial variation of temperature and Nusselt numbers for N_{re_i} = 3000

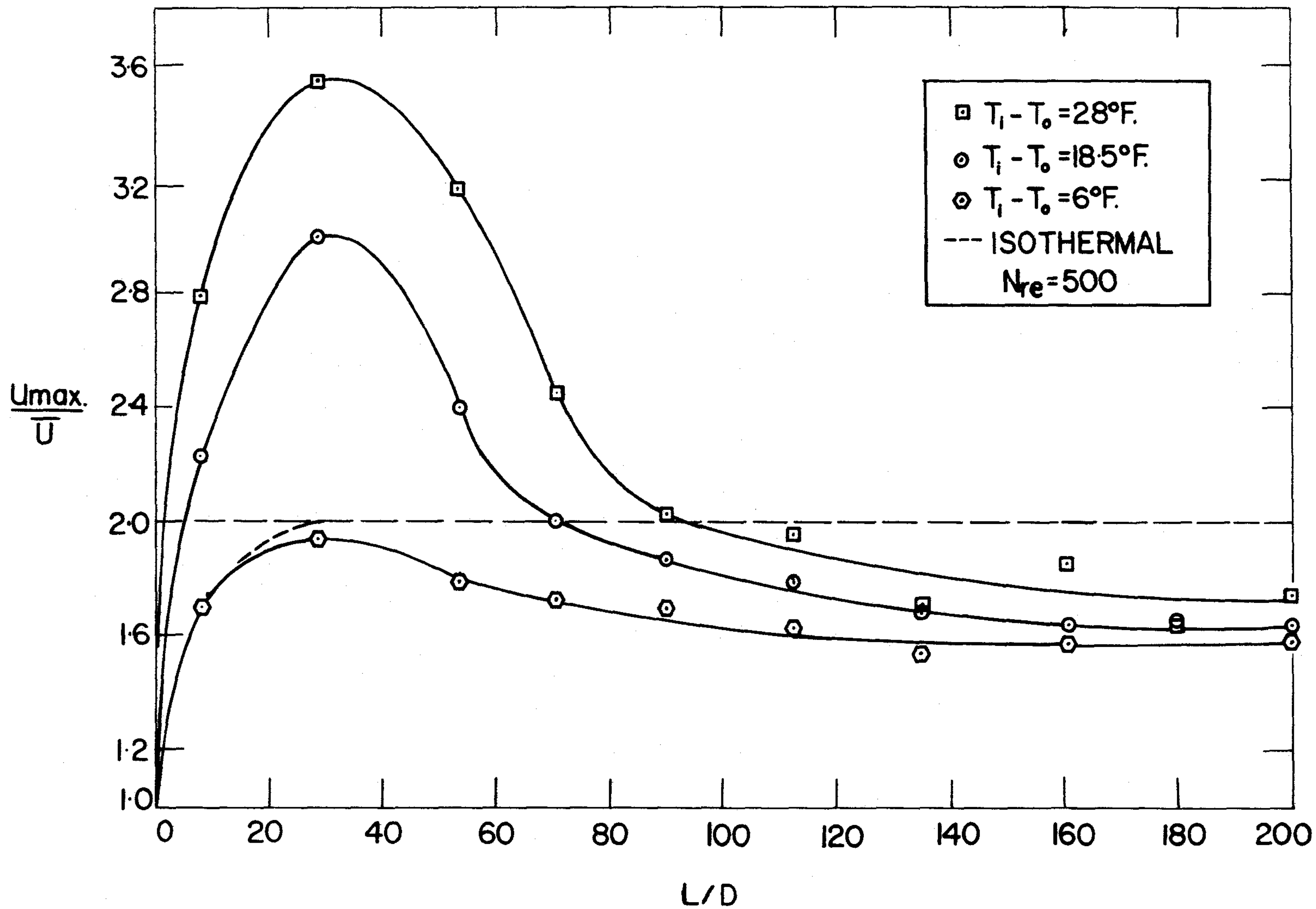

Fig. 6. Variation of $\frac{U_{max}}{\bar{U}}$ with $\frac{L}{D}$ for non-isothermal flow at $N_{re} = 500$.

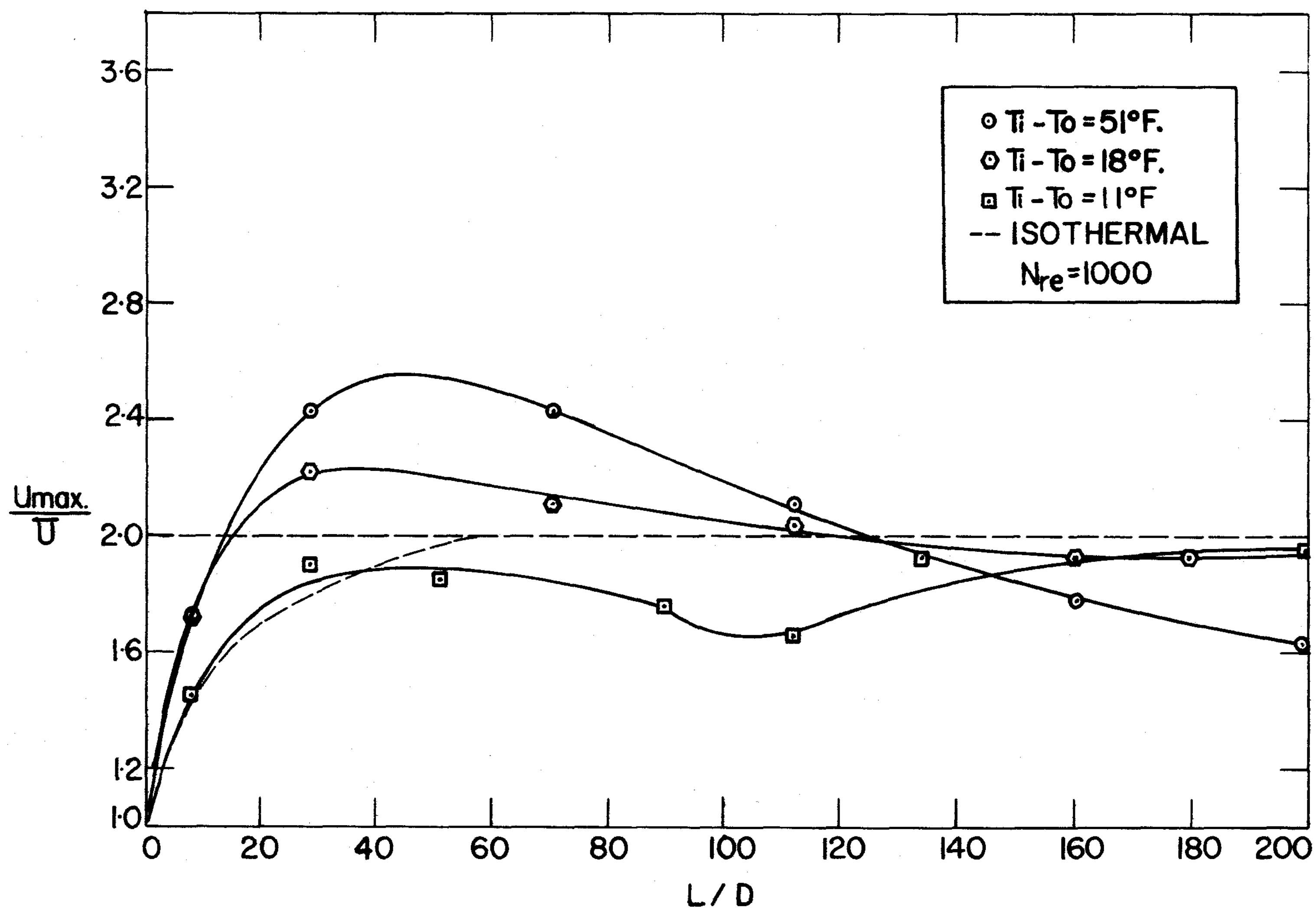

Fig. 7. Variation of $\frac{U_{max}}{\bar{U}}$ with $\frac{L}{D}$ for non-isothermal flow at N_{re}=1000

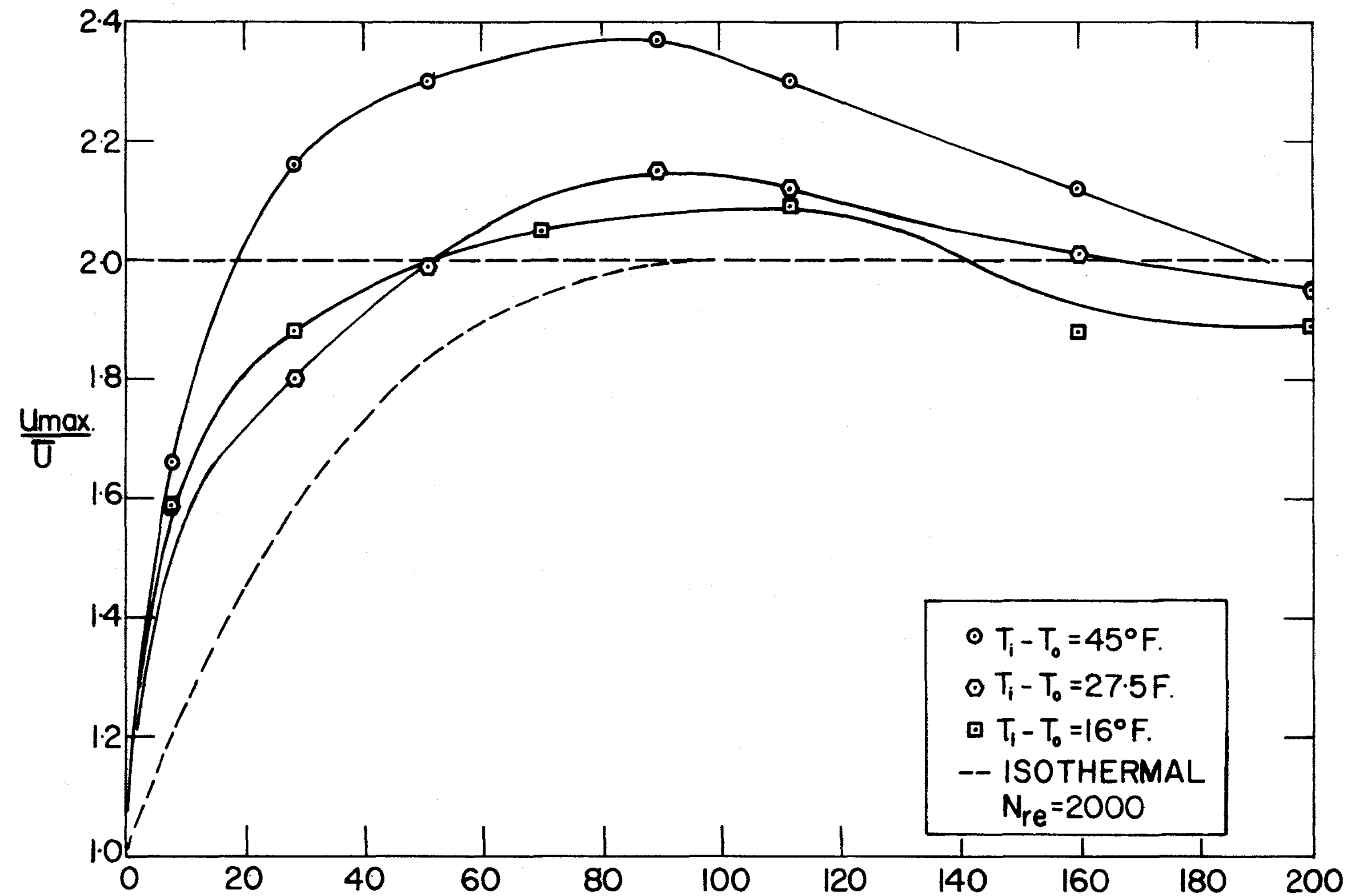

Fig. 8. Variation of $\frac{U_{max}}{\bar{U}}$ with $\frac{L}{D}$ for non-isothermal flow at N_{re}=2000

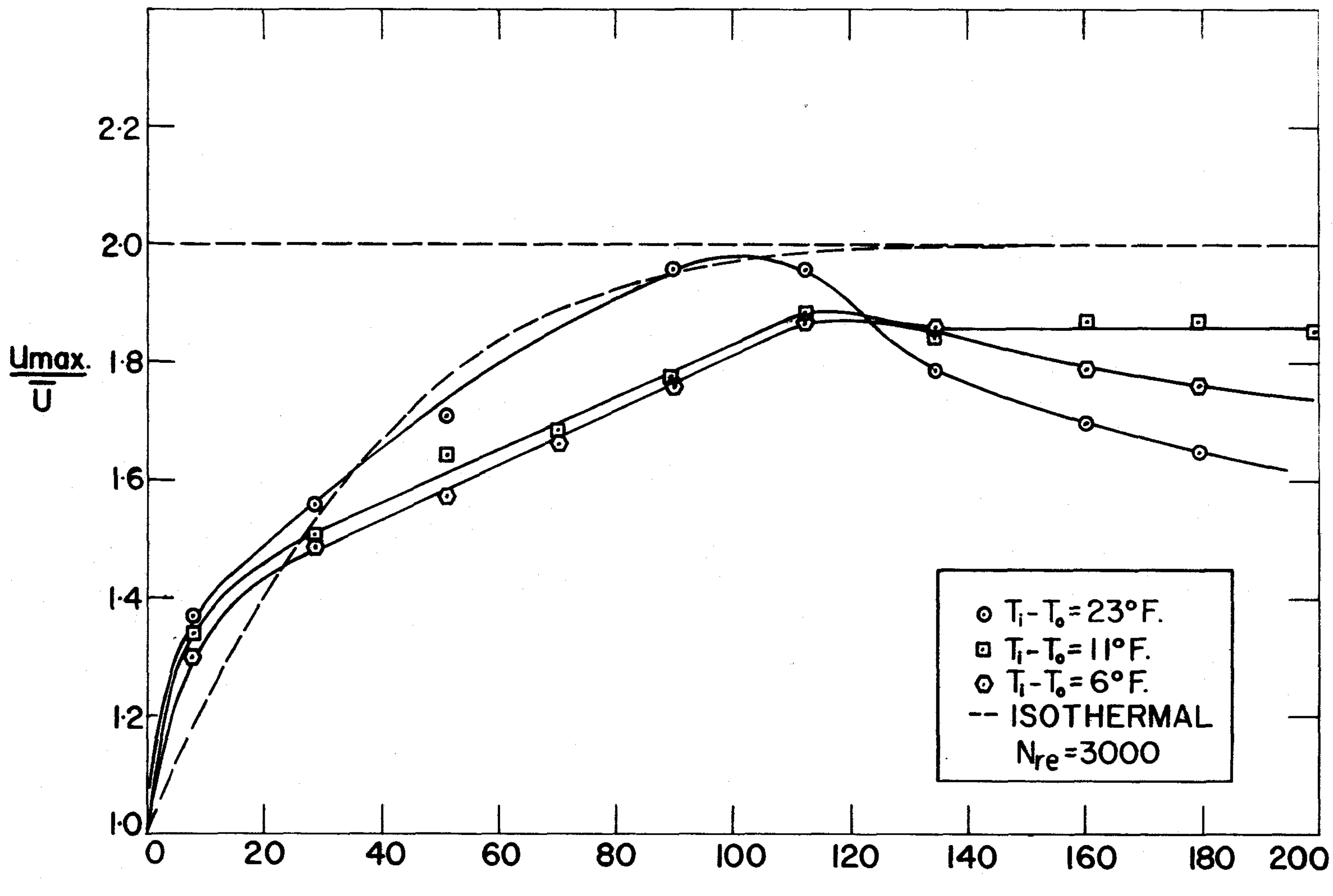

Fig. 9. Variation of $\frac{U_{max}}{\bar{U}}$ with $\frac{L}{D}$ for non-isothermal flow at $N_{re}=3000$

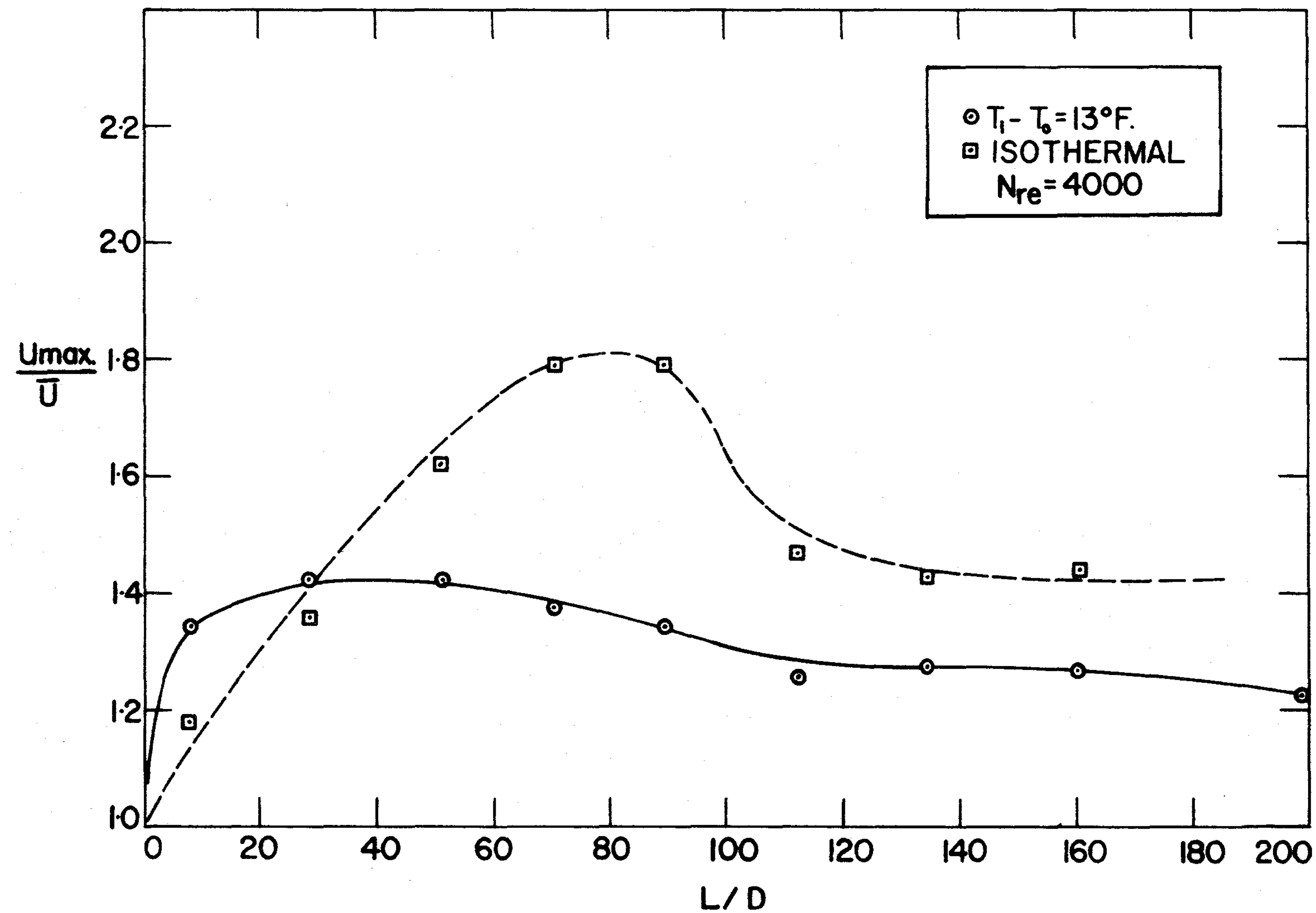

Fig. 10 Variation of $\frac{U_{max}}{\bar{U}}$ with $\frac{L}{D}$ for non-isothermal at $N_{re} = 4000$

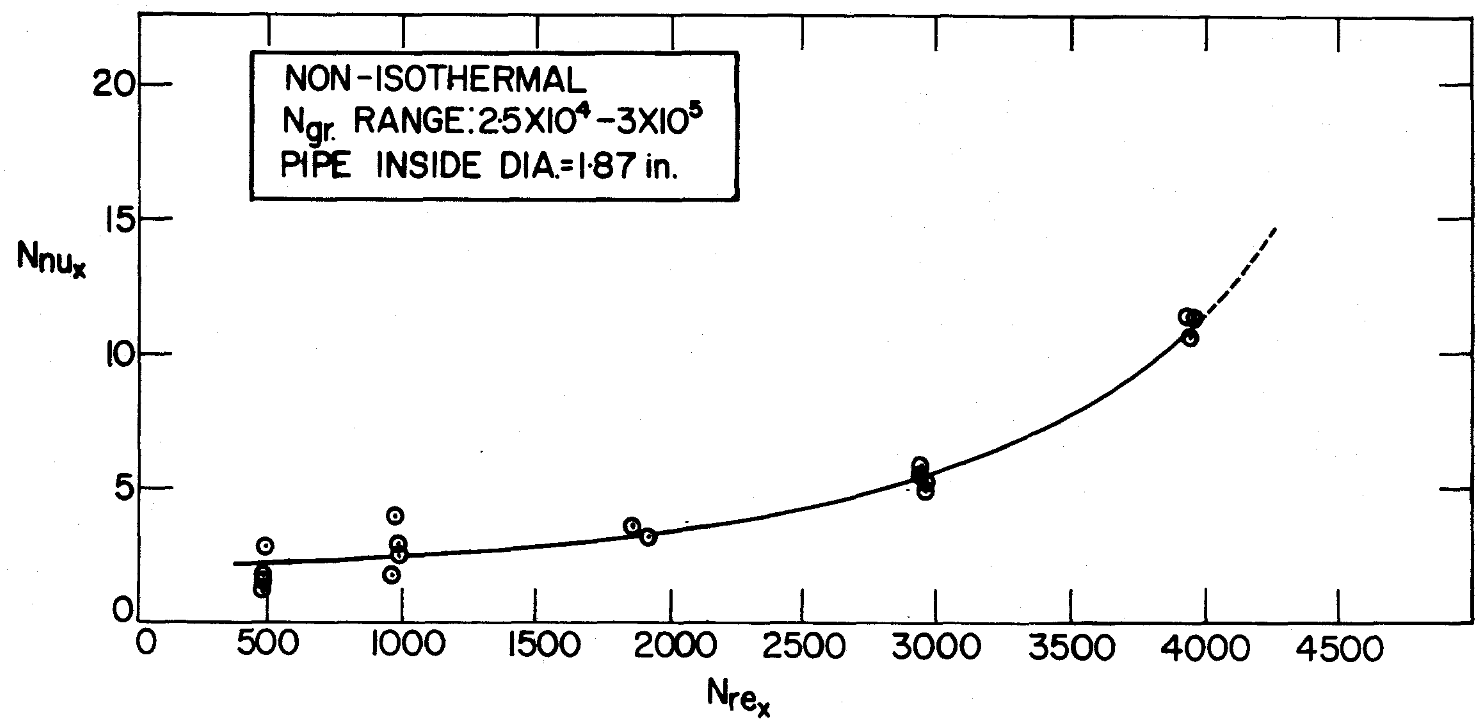

Fig. 11 Variation of N_{nu_x} with N_{re_x}

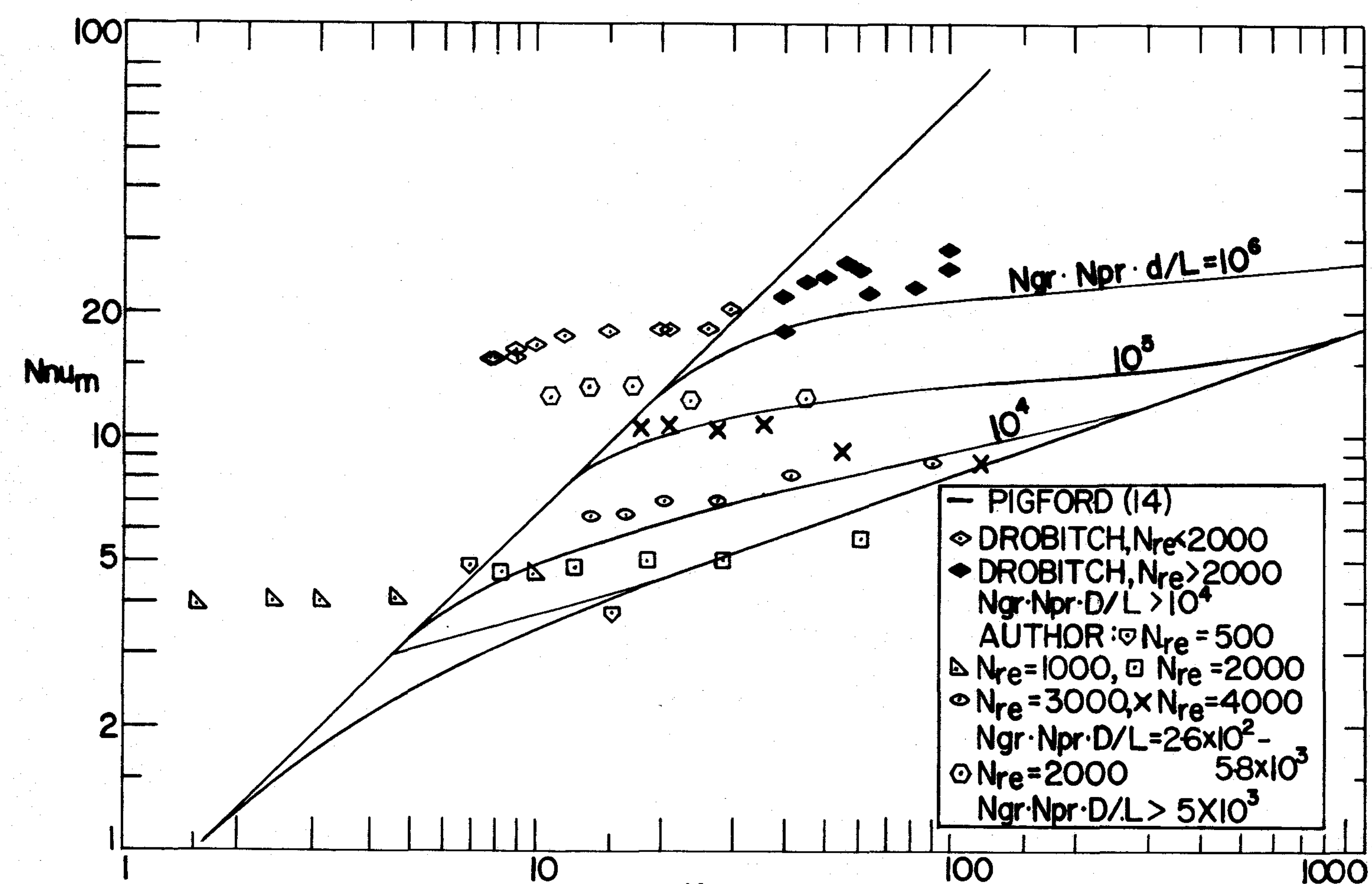

Fig. 12 Variation of Nnu_m with Ngz

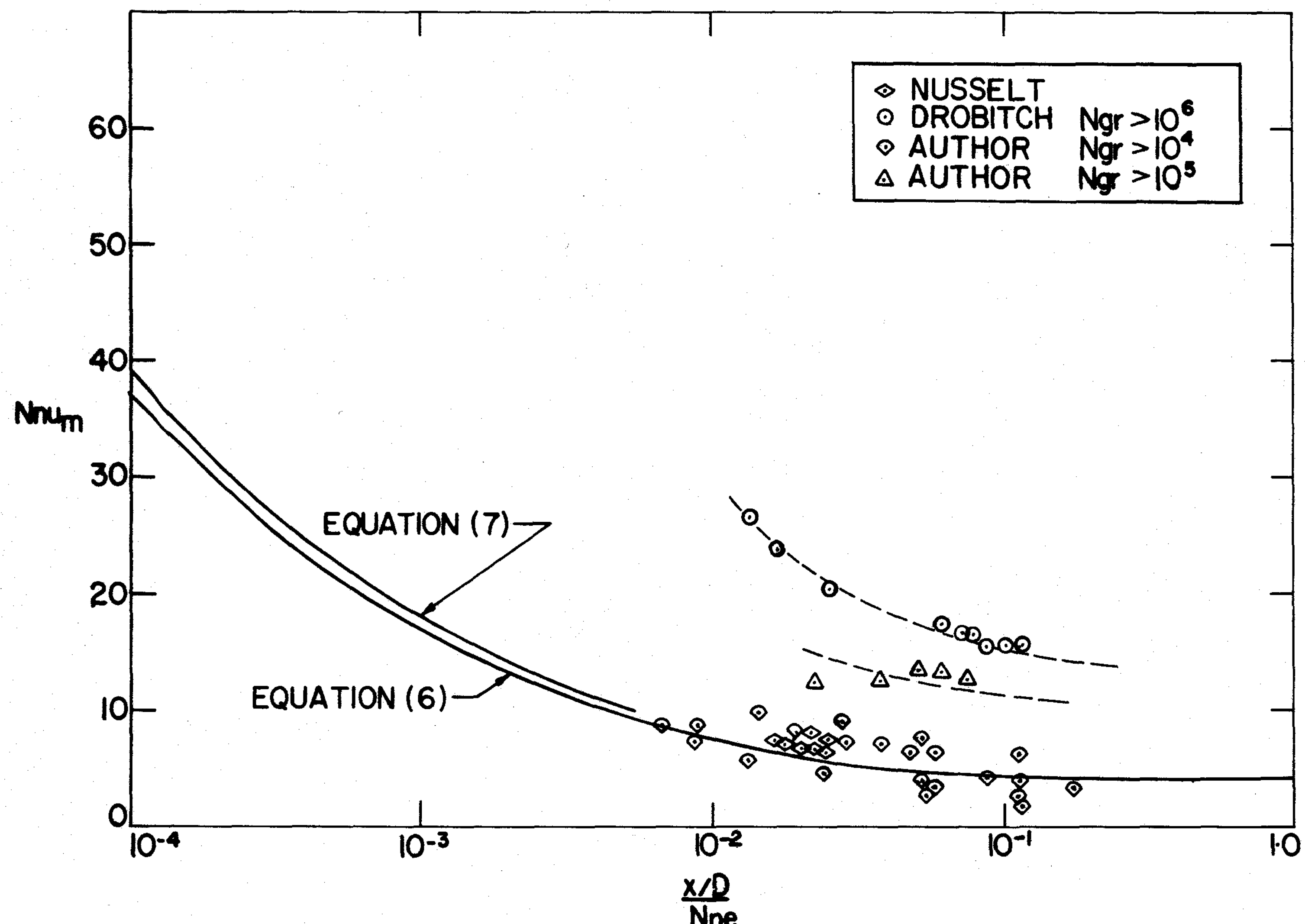

Fig. 13 Variation of Nnu_m with $\frac{x/D}{Npe}$

CHAPTER 5

DISCUSSION

Entrance Length

Figures 2 and 3 show the variation of entrance length with N_{Re}, and confirm the expression developed analytically by Langhaar

$$\frac{L}{D} = 0.0575\ N_{Re}$$

The present investigation deviates only 3% from this correlation up to a Reynolds number of 3000. Above this some turbulence was observed in the pipe which invalidates the above equation. When the Reynolds number is greater than 3200 the maximum velocity ratio $u_{max}/\ \overline{U}$ begins to decrease rapidly and results in a final value of 1.18 at $N_{Re} = 8000$.

Figure 3(a) shows the variation of Reynolds number with entrance length for isothermal and non-isothermal flow. The entrance length for non-isothermal flow was defined as the distance from the entrance to the point where the maximum velocity ratio ($u_{max}/\ \overline{U}$) occurred. It can be seen that for $N_{Re} < 1000$, the entrance length for isothermal and non-isothermal flow are approximately equal. For higher Reynolds numbers, the non-isothermal entrance length is smaller than for isothermal flow.

Axial Variation of Temperature

From figures 4 and 5 and Appendix C, it may be observed that the Reynolds number affects the mean and wall temperature in the same manner. Both decrease rapidly with axial distance for low Reynolds numbers but as the flow rate increases, the slope decreases and becomes very small for Reynolds numbers of 4000 or greater.

This effect complicates the study of heat transfer parameters at the low flow rates, unless the entrance temperature is high. For the present investigation accurate heat transfer results were difficult to obtain at low flow rates because isothermal conditions across the pipe were reached at low L/D ratios.

Velocity Ratio $u_{max}/ \overline{U}$

The isothermal part of this investigation confirms the velocity ratio of 2.0 for laminar and 1.2 for turbulent fully developed flow in a pipe as shown in figure 2.

Figures 6, 7, 8, 9 and 10 show the variation of $u_{max}/ \overline{U}$ with L/D ratios for non-isothermal flow at different temperature differences $(t_i - t_o)$ and various Reynolds numbers. The velocity ratio develops to well over 2.0 for most of the tests where $N_{Re} < 3000$. This is due to the buoyancy effects which elongate the profile. This increase in $u_{max}/ \overline{U}$ is most profound for the low mass flow rates where a maximum $u_{max}/ \overline{U}$ of 3.58 is obtained. For this test Reynolds number is 500 and the temperature difference is 28° F. For larger temperature differences at this mass flow this ratio will probably increase even further because the buoyancy effect will be more pronounced. As the mass flow increases, the buoyancy effect decreases and at Reynolds number of 4000, it becomes negligible and here inertial forces predominate.

From the same figures it may be noted that the velocity ratios quickly develop to a maximum, a point which coincides with the onset of isothermal fully developed laminar flow for $N_{Re} < 1000$. After this the profile becomes flatter and the flow becomes turbulent for all Reynolds numbers. When the flow across the section becomes isothermal again due to continuous cooling, the velocity ratio is expected to increase and the velocity profile will develop isothermally and become parabolic if the L/D ratio is large enough.

The velocity ratios decrease with increasing Reynolds numbers and decreasing temperatures for laminar flow, but when the Reynolds number becomes large (>3500), increasing temperature differences flatten the profile thus decreasing the velocity ratio.

Type of Flow

Isothermal flow is generally considered to be laminar when the Reynolds number is below 2300. The hot-wire anemometer indicated no turbulence for this mass flow, but above $N_{Re} = 2300$, it showed that turbulence was initiated and increased with Reynolds number.

For non-isothermal flow, the hot-wire anemometer indicated turbulence for Reynolds numbers as low as 500. This observation was also made by Drobitch (5) and Gulati (6). Turbulence may well be present at lower Reynolds numbers as Hanratty indicated with his investigation for water, where complete turbulence was found at $N_{Re} = 50$.

The fluctuations were due to variations of velocity and temperature. The oscilloscope and random signal voltmeter indicated high frequency velocity and low frequency temperature fluctuations, but no quantitative results could be obtained.

The hot-wire anemometer fluctuation increased

(1) with increasing mean temperature

(2) with decreasing velocity

(3) with distance from the center of the pipe.

Heat Transfer Characteristics

The variation of the heat transfer coefficients or local Nusselt numbers with L/D ratios is shown in figures 4 and 5 for Reynolds numbers of 500 and 3000 respectively. Data for other tests is given in Appendix C. Since the test stations were approximately three feet apart these 'local' Nusselt numbers are actually mean values for those sections. The Nusselt numbers are shown to decrease with L/D ratios for most Reynolds numbers and temperature differences. Those tests that do not show this trend are extremely low temperature runs, where the Nusselt number could not be obtained very accurately.

Figure 11 shows the variation of local Nusselt number with Reynolds number in the cooling region. Nusselt numbers are shown to increase with mass flow, but the variation of Grashof number was too small to determine whether it affects the Nusselt number. Figures 12 and 13, however, show that the Grashof number has a marked effect on the heat transfer coefficient.

In figure 12, the variation of mean Nusselt number with Graetz number is shown for data from the present investigation and also from Drobitch (5) and Pigford (14). It may be noted that the mean Nusselt number definitely increases with Grashof number or as Pigford suggested with Grashof modulus (N_{Gr} N_{Pr} D/L). Considering the results of the present investigation alone, it can only be concluded that the Nusselt number varies either with Reynolds and/or Grashof number, since only one pipe diameter was used. To investigate the effect of pipe diameter, one test was taken at N_{Re} = 2000 employing a high temperature difference (t_i = 400^{o}F). The results can be compared with Drobitch who had entrance temperatures close to 700^{o}F and a pipe diameter of 4.34". It may be noted that if the temperature differences had been the same, the mean Nusselt number would have been approximately the same. This indicates that diameter does not affect the relation between N_{Num} and N_{Gz}. The graph indicates that Reynolds number has some effect on the Nusselt number at low Grashof numbers as used in the present investigation. For the work of Drobitch, however, Reynolds number does not seem to affect the mean Nusselt number at all. Considering the tests at N_{Re} = 2000 for the lower Grashof numbers of this investigation ($N_{Gr} = 10^4$), the high temperature test ($N_{Gr} = 10^5$) and Drobitch ($N_{Gr} = 10^6$) it may be concluded that mean Nusselt numbers increase with Grashof number.

Figure 13 shows the variation of mean Nusselt number with $(x/d_w)/Pe$. Correlations obtained by Hausen and Seider and Tate are shown here, as well as experimental results of Nusselt, Drobitch and the present investigation. Hausen used constant wall temperature and a parabolic velocity distribution to obtain equation (6). Seider and Tate added the effect of variable viscosity using oil instead of air and developed equation (7). Hausen's equation seems to hold when the Grashof number is small, although he neglected all free convection effects. The mean Nusselt number increases with Grashof number as shown by the high temperature test and Drobitch. Hausen's correlation

$$N_{Num} = 3.66 + \frac{0.0668\ [(x/d_w)/Pe]^{-1}}{1 + 0.04\ [(x/d_w)/Pe]^{-2/3}}$$

should therefore include a Grashof number term to take its effect into consideration.

CHAPTER 6

CONCLUSIONS

All the heat transfer parameters and velocity ratios were calculated, and from the results the following conclusions were made:

(a) The relationship between entrance length and Reynolds number for isothermal flow developed by Langhaar (10) was confirmed to be

$$\frac{L'}{D} = 0.0575\ N_{Re} \qquad \text{within } 3\%.$$

(b) For non-isothermal flow, four distinct regions were observed as follows:

(1) Entrance region, from entrance to maximum $u_{max}/\ \overline{U}$.

(2) Cooling region, where the velocity ratio decreases continuously due to the cooling.

(3) Isothermal developing region. In this region, the effect of temperature difference has become negligible, and the velocity profile is developing isothermally.

(4) Fully developed laminar isothermal flow, which will continue if no disturbances are encountered.

(c) In the type of flow investigated in this work, the buoyancy force had the effect of elongating the velocity profile. The effect of this buoyancy force decreased with increasing Reynolds numbers.

(d) In region (2) or the cooling region the Nusselt number was noted to increase with Reynolds number.

(e) The air flow was of a turbulent nature for Reynolds numbers as low as 500, even when the temperature of the air flowing in the pipe was only a few degrees above the ambient air temperature.

(f) The mean Nusselt number variation with $(x/d_w)/Pe$ was found to agree with the correlation of Hausen

$$N_{Nu_m} = 3.66 + \frac{0.0668\ [(x/d_w)/Pe]^{-1}}{1 + 0.04\ [(x/d_w)/Pe]^{-2/3}}$$

when the Grashof number was between 10^4 - 10^5, but the Nusselt number increased with higher Grashof numbers and this term should be included in the equation.

BIBLIOGRAPHY

1. Boussinesque, J., Comptes Rendus 113, 9 and 49, (1891).

2. Chapman, A. J., Heat Transfer, The MacMillan Co., N. Y., (1960).

3. Deissler, R. G., Analytical Investigation of Fully Developed Laminar Flow in Tubes with Fluid Properties Variable Along the Radius, NACA Technical Note, No. 2410, (July 1951).

4. Deissler, R. G., Analytical Investigation of Turbulent Flow in Smooth Tubes with Heat Transfer with Variable Fluid Properties for Prandtl Number of 1, NACA Technical Note, No. 2242, (Dec. 1950).

5. Drobitch, A. J., Non-Isothermal Flow of Air in a Vertical Tube, An Experimental Study with the Hot-Wire Anemometer, M.A.Sc. Thesis, University of Windsor, Windsor, Ontario, (1965).

6. Gulati, U. S., Non-Isothermal Flow of Air in a Vertical Pipe at Low Velocities, M.A.Sc. Thesis, Assumption University of Windsor, Windsor, Ontario, (1963).

7. Hallman, T. M., Combined Forced and Free Laminar Heat Transfer in Vertical Tubes with Uniform Internal Heat Generation, ASME, Vol. 78, p. 1831, (1956).

8. Kays, W. M., A Summary of Experiments and Analysis for Gas Flow Heat Transfer and Friction in Circular Tubes, Technical Report No. 22, Dept. of Mech. Eng., Stanford Univ., (June 1954).

9. Knudsen, J. G., and Katz, D. L., Fluid Dynamics and Heat Transfer, McGraw-Hill Book Co., Inc., N. Y., (1959).

10. Langhaar, H. L., Steady Flow in the Transition Length of a Straight Tube, Journal of Applied Mechanics, Vol. 9, Trans. ASME, Vol. 64, p. A-55, (1942).

11. Martinelli, R. C., and Boelter, L. M. K., The Analytical Prediction of Superposed Free and Forced Viscous Convection in a Vertical Pipe, Univ. Calif. (Berkley) Publs. Eng., 5:23, (1942).

12. McAdams, W. H., Heat Transmission, McGraw-Hill Series in Chemical Engineering, N. Y., (1954).

13. Nicoll, W. B., and Kays, W. M., The Influence of Temperature Dependent Properties on Gas Flow Heat Transfer in Circular Tubes, Tech. Report No. 43, Dept. of Mech. Eng., Stanford University, California, (Sept. 1959).

14. Pigford, R. L., Non-Isothermal Flow and Heat Transfer Inside Vertical Tubes, Chem. Eng. Prog. Sym. Series, Vol. 51, No. 17, p. 79, (1953).

15. Rotta, J., Experimenteller Beitrag zur Entstehung Turbulenter Stromung im Rohr., Ing. Arch. 24, pp. 258 - 281, (1956).

16. Scheele, G. F., Rosen, E. M., and Hanratty, T. J., Effect of Natural Convection on Transition to Turbulence in Vertical Pipes, Can. Jour. Chem. Eng., Vol. 38, p. 67, (1960).

17. Scheele, G. F., and Hanratty, T. J., Effect of Natural Convection on

Stability of Flow in a Vertical Pipe, Jour. Fl. Mech., Vol. 14, pp. 244, (1962).

18. Schiller, L., Untursuchungen uber Laminare und Turbulente Stromung. Forschungsarb. a.d. Geb. Ing.-Wesen. Heft 248, ZAMM, 2, 96 or Phys. Z., 23, 14, (1922).

19. Seider, E. N., and Tate, G. E., Ind. Chem. Engrs., 31, 83 (1934).

20. Szewczyk, A. A., Combined Forced and Free - Convection Laminar Flow, ASME, Paper No. 63-WA-130, (1963).

21. Yamagata, K., A Contribution to the Theory of Non-Isothermal Laminar Flow of Fluids Inside a Straight Tube of Circular Cross-Section, Memoirs of the Faculty of Engineering, Kyushu Imperial University, Japan, Vol. 8, No. 6, pp. 365 - 449, (1940).

APPENDICES

APPENDIX A

HOT WIRE ANEMOMETER

The hot-wire anemometer has been used successfully for many years to obtain the velocity of fluids with a high degree of accuracy. If it is assumed that King's Equation (1) holds for values down to zero feet per second, no calibration is required other than obtaining two points, one at a high velocity and one in still air, since this is a linear relation.

$$u = \frac{C}{P}\left[\left(\frac{I1}{I_o}\right)^2 - 1.0\right]^2 \qquad (1)$$

where

I_o = the value of current in still air at a temperature T_o.

I_1 = the value of current at velocity u and at T_o.

C = calibration constant.

P = absolute static pressure.

Since, however, this equation did not agree with experimental results at low velocities (less than two feet per second) each wire was calibrated individually between zero and ten feet per second.

Figure 14 shows the relation between velocity and current graphically at resistance ratios of 1.2 and 1.4. A .0005 inch platinum wire was used in all the experimental work. In Table 1, the correction for current per each ten degrees Fahrenheit is listed. This is required for non-isothermal flow since the current capacity of the wire increases with temperature.

Table 1. Current Correction for Temperature

Resistance Ratio	1.2	1.4
Current Correction ma/10° F	.036	.055

It was noted that the hot-wire always indicated a higher than actual velocity. This was investigated in a pipe which at the measuring section contained laminar isothermal flow, the mass flow of which was known. By plotting the theoretical parabolic velocity profile and the experimental velocities as found by the anemometer on the same graph, it was noted that at the far wall the velocity indicated was much higher than the theoretical one and that the percentage of error decreased as the probe was traversed out of the pipe. The conclusion was reached that there was an area blockage effect due to the probe itself. Calculations showed that the necessary increase in velocity was concentrated around the probe and needles, thus resulting in erroneous readings far in excess of that expected due to the actual area blocked. This might be eliminated by bending the probe at a right angle near the end, thus positioning the hot-wire upstream of the probe where it would then indicate the correct reading. However, the problem of entering and leaving the pipe for this arrangement is complicated because the slightest vibration will break the hot-wire. Due to the fact that the pipe in which the hot-wire was calibrated was approximately the same diameter as the test pipe, the centerline velocity was quite accurate, because the error was included in the calibration. A graph of the distortion as recorded across the pipe section is shown in figure 15. This effect was taken into account in the actual velocity determination.

To obtain readings close to the wall, a third needle was constructed on the hot-wire anemometer probe. After the wire was soldered across its two needles, the distance between this wire and the tip of the third needle was measured under a microscope. This distance was kept at a minimum, in this case approximately .004". The third needle was part of an electrical circuit, which was completed when the extended tip established contact with the pipe wall.

It was noted however that this close to the wall, the air velocity was increased due to the gap effect created between the probe and the wall. The velocity values seriously exceeded their expected values up to a distance of approximately .012" from the wall. Between .012 and .020 the velocity would decrease again. At approximately .020 it coincided with the expected value and continued to move upwards along its predicted parabolic profile. This phenomena might also be improved by using the proposed bent probe.

If correct procedures are followed, the heat loss from the hot-wire due to conduction and by convection will automatically be included in the calibration. The loss by radiation can be shown to be negligible.

Although the theory of hot wire anemometry and the calibration procedures are well described in (5), it will be necessary to do more research to determine the effect of blockage if this arrangement is to be used accurately. If no suitable factor can be found to correct the velocity distortion, it may be necessary to turn to the proposed method above to obtain a higher degree of accuracy.

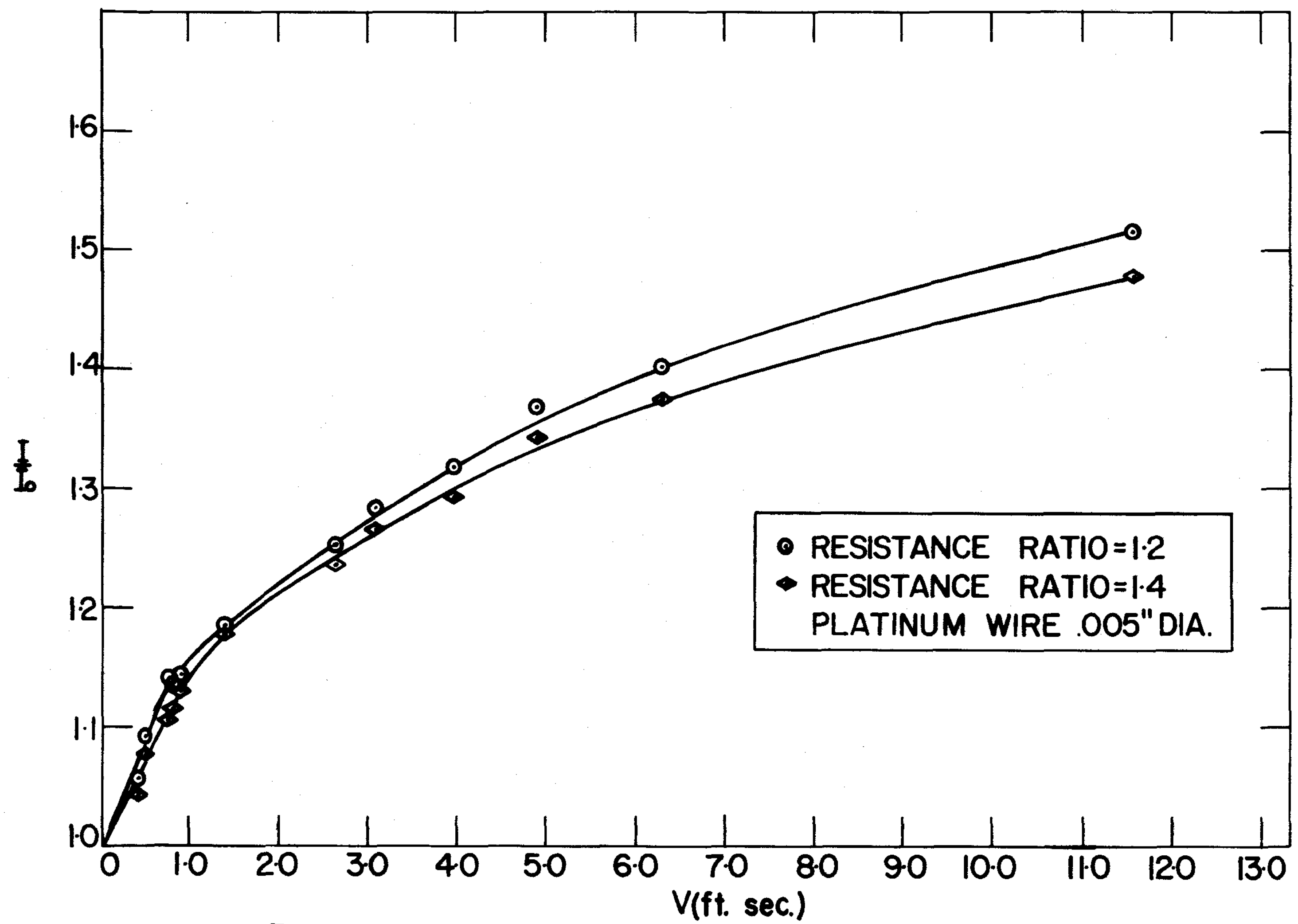

Fig. 14 Variation of I/Io with V for two resistance ratios

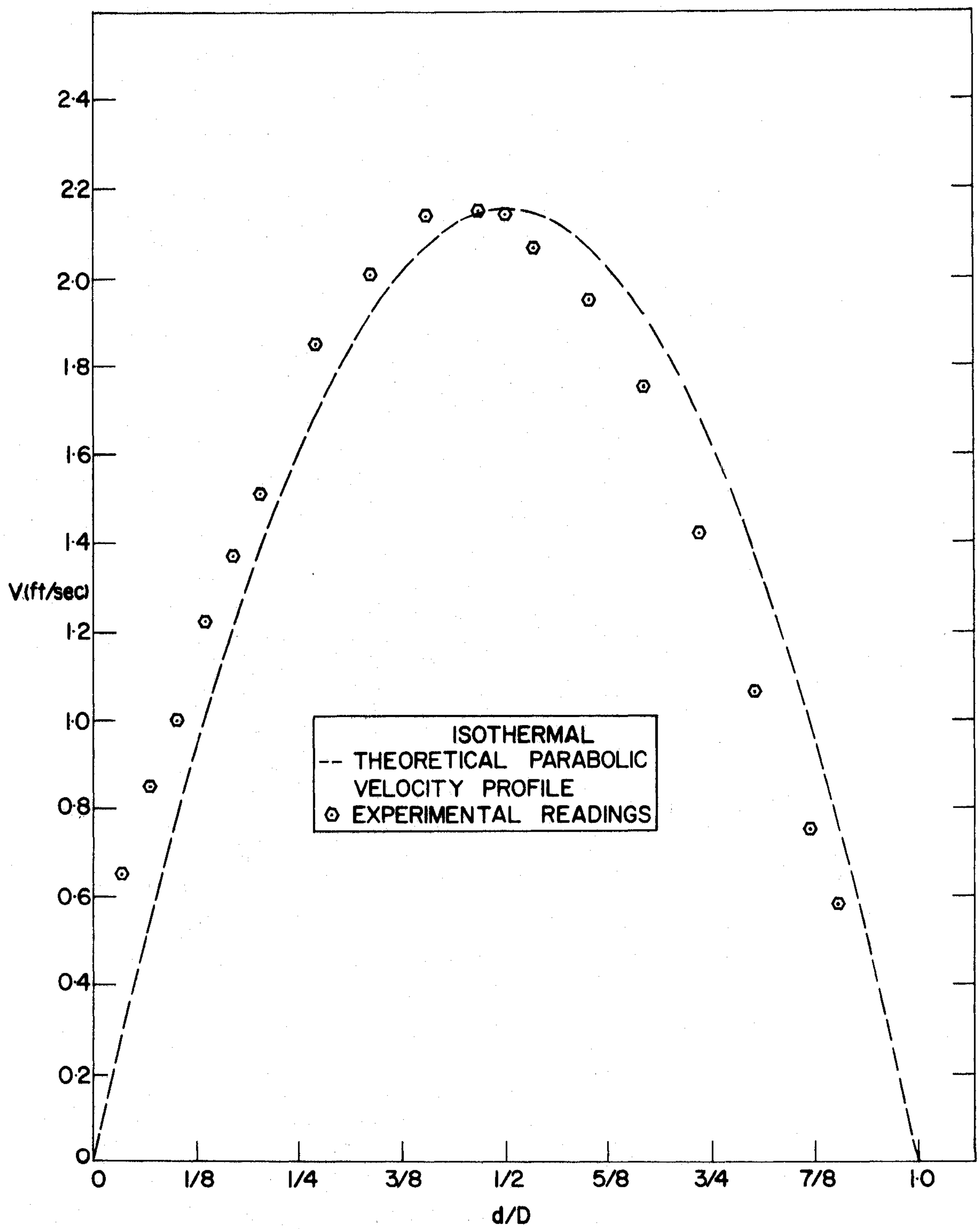

Fig. 15 Variation of V. with d/D for isothermal flow to show area blockage effect. Probe entrance is at right.

APPENDIX B

EVALUATION OF DIMENSIONLESS PARAMETERS

The dimensionless parameters used in this study were the following numbers: Grashof, Nusselt, Reynolds, Prandtl, Peclet and Graetz. This appendix will state how these numbers were evaluated.

Figure A shows a typical pipe section.

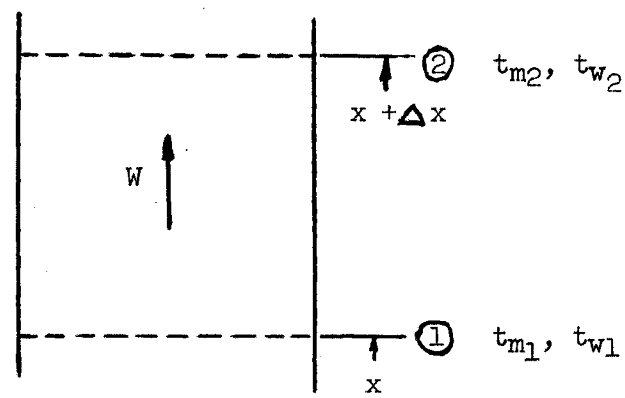

Figure A

(a) GRASHOF NUMBER

The Grashof number at the position x is defined by

$$N_{Gr_x} = \frac{D^3 \rho^2 g \beta \Delta T}{\mu^2}$$

where

$$\beta = \frac{1}{T_o} \quad (^oR)$$

$$\Delta T = T_{m1} - T_o \quad (^oR \text{ or } ^oF)$$

where ρ and μ are evaluated at T_{m1}.

(b) NUSSELT NUMBER

The Nusselt number will be considered local when it is the average Nusselt number between any two consecutive stations.

$$N_{Nu_x} = \frac{hD}{k}$$

where

$$h = \frac{W\ C_p(T_{m1} - T_{m2})}{A\ \Delta T}$$

therefore

$$N_{Nu_x} = \frac{W\ C_p(T_{m1} - T_{m2})\ D}{A\ \Delta T\ k}$$

where C_p and k are specific heat and conductivity respectively, evaluated at $\frac{T_{mx} + T_{mx}}{2}$ and the ΔT in the denominator is

$$\Delta T = \left(\frac{T_{m1} + T_{m2}}{2}\right) - \left(\frac{T_{w1} + T_{w2}}{2}\right)$$

The average or mean Nusselt number was defined as the following:

$$N_{Nu_m} = \frac{1}{L}\int_0^L N_{Nu_x}\, dx$$

(c) REYNOLDS NUMBER

The Reynolds number at any position x is given by

$$N_{Re_x} = \frac{\rho_x\ D\ \bar{U}_x}{\mu_x}$$

where ρ_x, μ_x and $\bar{U}_x$ are determined at T_m.

When the Reynolds number is used in the evaluation of the Peclet and Graetz numbers it is based on the average temperature between the two positions, i.e.

$$T = \frac{T_{m1} + T_{m2}}{2}$$

(d) PRANDTL NUMBERS

The Prandtl number defined as $\frac{C_p\mu}{k}$ was assumed to be constant at 0.71.

(e) MEAN TEMPERATURE

All mean temperatures were determined from the following equation:

$$T_m = \frac{1}{r_o}\int_0^{r_o} t\ r\ dr$$

which agreed well with the following equation for bulk temperature.

$$T_b = \frac{\int_0^{r_o} C_p\ T\ u\ r\ dr}{\int_0^{r_o} C_p\ u\ r\ dr}$$

Since all other dimensionless parameters used are functions of the preceding, they need not be discussed here.

APPENDIX C

Table C-1. Variation of Temperature and Dimensionless Parameters with L/D Ratio.

<u>Run No. 1</u>

Barometric Pressure	- 29.46" Hg.
Ambient Air Temperature	- 70.0°F.
Weight Flow	- 2.704 lbs/hr
Mean Nusselt No.	- 5.065

L/D	t_m °F	t_w °F	N_{Re}	N_{Nu}	N_{Gr} x 10^{-4}	$u_{max}/\overline{U}$
0	76.0		491			
8.02	73.81	71.3	494	7.87	4.12	1.70
28.88	71.08	70.6	499	2.26	1.17	1.94
51.34	70.15	70.3	500		.163	1.79
70.59	70.0	70.2	501		.642	1.73
89.84	70.0	70.0	501			1.70
112.30	70.0	70.0	501			1.62
134.76	70.0	70.0	501			1.52
160.43	70.0	70.0	501			1.56
179.68	70.0	70.0	501			1.43
198.93	70.0	70.0	501			1.58
218.18	70.0	70.0	501			1.49

Table C-2. Variation of Temperatures and Dimensionless Parameters with L/D Ratio.

Run No. 2		
	Barometric Pressure	- 29.46" Hg.
	Ambient Air Temperature	- 69.0°F.
	Weight Flow	- 2.704 lbs/hr
	Mean Nusselt No.	- 5.22

L/D	t_m $^{\circ}$F	t_w $^{\circ}$F	N_{Re}	N_{Nu}	N_{Gr} x 10^{-4}	$u_{max}/\bar{U}$
0	87.5					
8.02	82.9	75.5	479		13.78	2.23
				3.78		
28.88	78.0	74.2	487		10.87	3.00
				6.18		
51.34	75.0	73.0	492		7.95	2.40
				9.47		
70.59	74.2	72.0	493		6.14	2.00
				1.81		
89.84	73.1	72.0	495		5.06	1.87
				3.02		
112.30	72.5	72.0	496			1.79
134.76	72.0	72.0	497			1.68
160.43	72.0	72.0	497			1.64
179.68	72.0	72.0	497			1.66
198.93	72.0	72.0	497			1.64
218.18	72.0	72.0	497			1.50

Table C-3. Variation of Temperatures and Dimensionless Parameters with L/D Ratio.

<u>Run No. 3</u>

	Barometric Pressure	- 29.58" Hg.
	Ambient Air Temperature	- 73.0°F.
	Weight Flow	- 2.821 lbs/hr
	Mean Nusselt No.	- 1.71

L/D	t_m °F	t_w °F	N_{Re}	N_{Nu}	N_{Gr} x 10^{-4}	$u_{max}/\overline{U}$
0	100.0					
8.02	91.3	77.0	469		17.89	2.79
				2.67		
28.88	83.9	73.5	480		10.61	3.55
				1.43		
51.34	79.8	73.2	487		6.64	3.17
				1.49		
70.59	77.9	73.0	490		6.00	2.45
				1.63		
89.84	76.5	73.0	492		4.67	2.03
112.30	75.3	73.0	494			1.96
134.76	74.2	73.0	496			1.71
160.43	73.0	73.0	498			1.86
179.68	73.0	73.0	498			1.65
198.93	73.0	73.0	498			1.75
218.18	73.0	73.0	498			1.52

Table C-4. Variation of Temperatures and Dimensionless Parameters with L/D Ratio.

<u>Run No. 4</u>

Barometric Pressure	- 29.50" Hg.
Ambient Air Temperature	- 82.5°F.
Weight Flow	- 5.52 lbs/hr
Mean Nusselt No.	- 1.50

L/D	t_m °F	t_w °F	N_{Re}	N_{Nu}	N_{Gr} x 10^{-4}	$u_{max}/\bar{U}$
0	100.5					
8.02	97.3	84.3	951	1.44	13.12	1.71
28.88	95.1	83.5	959	1.09	11.64	2.22
51.34	93.6	83.0	963	2.39	10.46	2.17
70.59	91.1	82.5	970		8.47	2.12
89.84	88.6	82.5	978			2.09
112.30	84.1	82.5	993			2.04
134.76	82.5	82.5	998			1.98
160.43	82.5	82.5	998			1.93
179.68	82.5	82.5	998			1.93
198.93	82.5	82.5	998			1.92
218.18	82.5	82.5	998			1.91

Table C-5. Variation of Temperatures and Dimensionless Parameters with L/D Ratio.

<u>Run No. 5</u>

Barometric Pressure - 29.40" Hg.

Ambient Air Temperature - 70.1°F.

Weight Flow - 5.32 lbs/hr

Mean Nusselt No. - 3.44

L/D	t_m °F	t_w °F	N_{Re}	N_{Nu}	N_{Gr} x 10^{-4}	$u_{max}/\bar{U}$
0	100.1		909			
8.02	92.3	76.8	931		19.8	1.98
				4.69		
28.88	84.6	73.0	955		13.67	2.46
				3.38		
51.34	80.4	71.9	968		9.93	2.70
				4.03		
70.59	77.2	70.9	978		6.97	2.66
				3.97		
89.84	75.0	70.0	985		4.94	2.20
				1.98		
112.30	73.9	70.0	989		3.87	2.18
				3.15		
134.76	72.8	70.0	992		2.80	1.98
160.43	71.4	70.0	997			1.91
179.68	70.0	70.0	1002			1.74
198.93	70.0	70.0	1002			1.67
218.18	70.0	70.0	1002			1.54

Table C-6. Variation of Temperatures and Dimensionless Parameters with L/D Ratio.

Run No. 6 Barometric Pressure - 29.26" Hg.

Ambient Air Temperature - 70.5^{o}F.

Weight Flow - 10.81 lbs/hr

Mean Nusselt No. - 7.564

L/D	t_m ^{o}F	t_w ^{o}F	N_{Re}	N_{Nu}	N_{Gr} x 10^{-4}	$u_{max}/\overline{U}$
0	86.5					
8.02	80.6	72.8	1941		12.89	1.60
				5.63		
28.88	77.3	71.2	1959		8.77	1.88
				7.14		
51.34	76.9	71.2	1962		5.86	1.99
				7.52		
70.59	75.0	71.2	1974		3.56	2.05
				10.78		
89.84	72.9	70.5	1987		0.42	2.04
112.30	71.0	70.5	2005			2.09
134.76	70.5	70.5	2005			
160.43	70.5	70.5	2005			1.88
179.68	70.5	70.5	2005			
198.93	70.5	70.5	2005			1.89
218.18	70.5	70.5	2005			1.87

Table C-7. Variation of Temperatures and Dimensionless Parameters with L/D Ratio.

<u>Run No. 7</u>

Barometric Pressure	-	29.60" Hg.
Ambient Air Temperature	-	70.2°F.
Weight Flow	-	10.71 lbs/hr
Mean Nusselt No.	-	5.00

L/D	t_m °F	t_w °F	N_{Re}	N_{Nu}	N_{Gr} x 10^{-4}	$u_{max}/\bar{U}$
0	97.7		1847			
8.02	92.4	75.0	1865		21.89	1.59
				3.67		
28.88	89.0	74.0	1885		19.23	1.80
				5.93		
51.34	84.3	73.0	1915		15.33	1.99
				6.91		
70.59	80.5	71.0	1941		12.12	2.01
				2.67		
89.84	79.3	70.7	1946		10.4	2.15
				5.30		
112.30	76.9	70.5	1962		8.82	2.12
134.76	74.3	70.2	1978			2.07
160.43	72.6	70.2	1990			2.01
179.68	70.2	70.2	2008			1.79
198.93	70.2	70.2	2008			1.82
218.18	70.2	70.2	2008			1.90

Table C-8. Variation of Temperatures and Dimensionless Parameters with L/D Ratio.

<u>Run No. 8</u>

Barometric Pressure	- 29.37" Hg.
Ambient Air Temperature	- 72.5°F.
Weight Flow	- 10.84 lbs/hr
Mean Nusselt No.	- 4.61

L/D	t_m °F	t_w °F	N_{Re}	N_{Nu}	N_{Gr} x 10^{-4}	$u_{max}/\bar{U}$
0	117.5					
8.02	104.7	83.6	1793		28.86	1.66
				5.75		
28.88	97.9	78.5	1832		23.64	2.16
				4.37		
51.34	93.1	77.1	1861		19.73	2.30
				5.00		
70.59	89.1	75.5	1885		16.70	2.30
				2.14		
89.84	87.6	74.6	1894		15.46	2.37
112.30	83.3	73.8	1921		12.59	2.30
				4.31		
134.76	81.7	72.5	1931			2.21
160.43	78.7	72.5	1948			2.12
179.68	75.8	72.5	1968			2.11
198.93	73.9	72.5	1981			
218.18	72.5	72.5	1990			1.79

Table C-9. Variation of Temperatures and Dimensionless Parameters with L/D Ratio.

Run No. 9 — Barometric Pressure - 29.85" Hg.

Ambient Air Temperature - 69.0°F.

Weight Flow - 15.94 lbs/hr

Mean Nusselt No. - 5.41

L/D	t_m °F	t_w °F	N_{Re}	N_{Nu}	N_{Gr} x 10^{-4}	$u_{max}/\bar{U}$
0	91.9					
8.02	87.5	71.9	2837		20.15	1.37
				5.53		
28.88	84.6	70.7	2864		17.34	1.56
				5.57		
51.34	81.9	70.0	2889		14.65	1.71
				6.39		
70.59	79.6	69.7	2911		12.35	1.69
				3.44		
89.84	78.4	69.4	2922		11.25	1.81
				7.62		
112.30	76.0	69.1	2945		8.90	1.96
				3.35		
134.76	75.2	69.0	2953		8.05	1.79
				6.64		
160.43	73.5	69.0	2970		6.37	1.70
179.68	72.4	69.0	2981		5.26	1.65
198.93	72.4	69.0	2981		5.31	1.80
218.18	72.0	69.0	2985			1.78

Table C-10. Variation of Temperatures and Dimensionless Parameters with L/D Ratio.

Run No. 10   Barometric Pressure - 29.51" Hg.

Ambient Air Temperature - 71.0°F.

Weight Flow - 15.97 lbs/hr

Mean Nusselt No. - 6.26

L/D	t_m °F	t_w °F	N_{Re}	N_{Nu}	N_{Gr} x 10^{-4}	$u_{max}/\bar{U}$
0	83.0					
8.02	80.9	75.0	2898		10.08	1.31
				8.75		
28.88	78.9	74.0	2918		8.38	1.56
				7.54		
51.34	77.4	73.1	2932		6.90	1.51
				5.13		
70.59	76.5	71.3	2941		6.00	1.70
				6.71		
89.84	75.4	71.0	2951		4.77	1.70
				4.58		
112.30	74.6	71.0	2959		4.07	1.52
				5.90		
134.76	73.8	71.0	2967		3.24	1.86
160.43	71.8	71.0	2987			1.47
179.68	71.0	71.0	2999			1.78
198.93	71.0	71.0	2999			1.83
218.18	71.0	71.0	2999			1.75

Table C-11. Variation of Temperatures and Dimensionless Parameters with L/D Ratio.

<u>Run No. 11</u>

Barometric Pressure	-	29.32" Hg.
Ambient Air Temperature	-	74.0°F.
Weight Flow	-	15.93 lbs/hr
Mean Nusselt No.	-	8.18

L/D	t_m °F	t_w °F	N_{Re}	N_{Nu}	N_{Gr} x 10^{-4}	$u_{max}/\overline{U}$
0	80.0					
8.02	78.8	75.3	2952		4.64	1.34
				7.16		
28.88	77.9	75.1	2959		3.77	1.51
				7.79		
51.34	77.1	75.0	2968		2.98	1.64
				10.06		
70.59	76.4	74.5	2975		2.34	1.68
89.84	75.1	74.0	2988			1.77
112.30	74.0	74.0	2999			1.88
134.76	74.0	74.0	2999			1.84
160.43	74.0	74.0	2999			1.87
179.68	74.0	74.0	2999			1.87
198.93	74.0	74.0	2999			1.85
218.18	74.0	74.0	2999			1.89

Table C-12. Variation of Temperatures and Dimensionless Parameters with L/D Ratio.

<u>Run No. 12</u>

Barometric Pressure	-	29.42" Hg.
Ambient Air Temperature	-	70.0°F.
Weight Flow	-	5.11 lbs/hr
Mean Nusselt No.	-	10.92

L/D	t_m °F	t_w °F	N_{Re}	N_{Nu}	N_{Gr} x 10^{-4}	$u_{max}/\overline{U}$
0	83.0					
8.02	80.9	74.8	3864		10.80	1.34
				8.62		
28.88	79.4	73.0	3884		9.23	1.43
				9.98		
51.34	77.6	72.7	3908		7.47	1.43
				13.95		
70.59	75.9	71.7	3929		5.77	1.38
				8.90		
89.84	74.9	71.4	3941		4.85	1.34
				12.36		
112.30	73.7	70.9	3957		3.63	1.25
				10.32		
134.76	72.9	70.6	3969		2.81	1.28
160.43	71.0	70.0	3992			1.26
179.68	70.0	70.0	4005			1.34
198.93	70.0	70.0	4005			1.22
218.18	70.0	70.0	4005			1.19

VITA AUCTORIS

1940 Born in Schyndel, N. B., Holland on April 24.

1959 Finished High School. (Saint Peter's High School in Peterborough, Ontario).

1962 Received a Diploma in Engineering from Saint Mary's University in Halifax, Nova Scotia.

1964 Received the Bachelor's Degree in Mechanical Engineering from Nova Scotia Technical College in Halifax, Nova Scotia.

1965 Candidate for the Degree of Master of Applied Science in Mechanical Engineering at the University of Windsor, Windsor, Ontario.